The Genesis of the Hashitu Porphyry Molybdenum Deposit, Inner Mongolia, NE China: Constraints from Mineralogical, Fluid Inclusion and Multiple Isotope (H, O, S, Mo, Pb) Studies

Degao Zhai[1*], Jiajun Liu[1], Stylianos Tombros[2], Anthony E. Williams-Jones[3]

[1]*State Key Laboratory of Geological Processes and Mineral Resources, China University of Geosciences, Beijing, 100083, China*

[2]*Department of Geology, University of Patras, Rion, 26500, Patras, Hellas*

[3]*Department of Earth and Planetary Sciences, McGill University, 3450, Quebec, Canada*

Corresponding author: D. Zhai, dgzhai@cugb.edu.cn

State Key Laboratory of Geological Processes and Mineral Resources, China University of Geosciences, Beijing, 100083, China

Submitted to: *Mineralium Deposita*

19th, May, 2016

Zhai, D. G., J. J. Liu, S. Tombros, and A. E. Williams-Jones. "The Genesis of the Hashitu Porphyry Molybdenum Deposit, Inner Mongolia, Ne China: Constraints from Mineralogical, Fluid Inclusion, and Multiple Isotope (H, O, S, Mo, Pb) Studies." Mineralium Deposita 53, no. 3 (Mar 2018): 377-97. http://dx.doi.org/10.1007/s00126-017-0745-5.

Abstract

The Hashitu porphyry molybdenum deposit is a newly-discovered Climax-type Mo deposit in the Great Hinggan Range Cu-Mo-Pb-Zn-Ag polymetallic metallogenic province of NE China, in which the Mo-bearing quartz veins are hosted in approximately coeval granites and porphyries. The deposit contains more than 100 Mt of ore with an average grade of 0.13 wt. % Mo. This well-preserved magmatic-hydrothermal system provides an excellent opportunity to determine the source of the molybdenum, the evolution of the hydrothermal fluids and the controls on molybdenite precipitation in a potentially important but poorly understood metallogenic province. Studies of fluid inclusions hosted in quartz veins demonstrate that the Hashitu hydrothermal system evolved to progressively lower pressure and temperature. Mineralogical and fluid inclusion analyses, and physiochemical calculations suggest that molybdenite deposition occurred at a temperature of 285º to 325 ºC, a pressure from 80 to 230 bars, a pH from 3.5 to 5.6, and a log fO_2 from -3 to +2 log units below and above the hematite-magnetite buffer, respectively. Results of multiple isotope (O, H, S, Mo and Pb) analyses are consistent in indicating a genetic relationship between the ore-forming fluids, metals and the Mesozoic granitic magmatism. Temperature and pressure decreases are inferred to have been the causes of molybdenite precipitation. The Hashitu porphyry molybdenum deposit is similar to other Climax-type Mo deposits, characteristics of which may be helpful for targeting other Hashitu-type deposits.

Key words: Fluid Inclusions; Mo Isotopes; Porphyry Mo Deposits; Hashitu; Northeast China

Introduction

Climax-type porphyry molybdenum deposits are relatively uncommon. The main examples of these deposits are Climax, Henderson, Mount Emmons, Silver Cliff, Pine Grove, Questa and Mount Hope in the USA and Nordli in Norway (White et al., 1981). They are invariably emplaced in post-subduction extensional settings, and the associated intrusions are commonly A-type granitoids. Usually, the molybdenum mineralization occurs in the form of quartz-molybdenite stockworks located within or proximal to F-, Rb-, Nd- and Ta-enriched A-type granitic cupolas (Ludington and Plumlee, 2009). Economic Climax-type deposits typically contain between 100 and 1000 Mt of ore grading between 0.1 and 0.3 % Mo; F > 2000, Rb > 250, Nb > 20, Ta > 2, Sr <100 and Zr <120 ppm (White et al., 1981; Keith et al., 1993). They are enriched in Be, Cs, Li, Sn, Th, and W, but

Zhai, D. G., J. J. Liu, S. Tombros, and A. E. Williams-Jones. "The Genesis of the Hashitu Porphyry Molybdenum Deposit, Inner Mongolia, Ne China: Constraints from Mineralogical, Fluid Inclusion, and Multiple Isotope (H, O, S, Mo, Pb) Studies." Mineralium Deposita 53, no. 3 (Mar 2018): 377-97. http://dx.doi.org/10.1007/s00126-017-0745-5.

depleted in Cu. However, numerous aspects of their genesis, including the source of the metals of economic interest, the processes responsible for molybdenum ore-formation and the tectonic settings for their emplacement, are still debated (Richards 2003; Seedorff and Einaudi 2004; Audétat 2015).

The Hashitu Mo deposit, which is located in the southern segment of the Great Hinggan Range and easternmost part of the Central Asian Orogenic belt in NE China, is the first "Climax-type" deposit to have been discovered in NE China. It is hosted by a late Jurassic A-type granite of the same name, interpreted to have been emplaced in a back arc tectonic setting, and contains more than 100 Mt of Mo ore, with an average grade of 0.13 wt.% Mo. The ore bodies are mainly in the form of quartz-molybdenite veins and stockworks that are concentrated largely in the apical parts of the pluton. This deposit formed during the late Jurassic (molybdenite Re-Os age, 147 ± 1 Ma), and is very similar in age to the host granites and porphyries (zircon U-Pb ages, 143 ± 2 to 147 ± 1 Ma) (Zhai et al. 2014a).

In this contribution, we report results of a comprehensive investigation of the Hashitu Mo deposit using mineralogical, multiple isotopic (H, O, S, Mo and Pb) and fluid inclusion methods. These results are used to determine the source, nature and evolution of the ore fluid, the source of the metals, and the physicochemical conditions and controls of molybdenite deposition. The study also examines the differences between the Hashitu Mo deposit and other Climax-type Mo deposits and the causes for these differences.

The Great Hinggan Range Metallogenic Belt

The Hashitu Mo deposit occurs in the Great Hinggan Range (GHR) Metallogenic Belt, which lies in the easternmost part of the Central Asian Orogenic Belt (labeled as CAOB in Fig. 1a). The CAOB is rimmed by the Siberian, Tarim and North China Cratons (labeled as SC, TC and NCC in Fig. 1a). This region is marked by the widespread occurrence of Mesozoic volcanic and intrusive rocks (Fig. 1b and c), including I- and A-type plutons, which were emplaced in four successive stages of geotectonic evolution (Xiao et al., 2004; Wu et al., 2004, 2005). An early phase of crustal accretion took place in the Neoproterozoic to Paleozoic, and was related to the subduction of the Paleo-Asian oceanic plate. This was followed by uplift in response to collision in the early Mesozoic. During the Late Jurassic, collision was succeeded by subduction of the Paleo-Pacific

Zhai, D. G., J. J. Liu, S. Tombros, and A. E. Williams-Jones. "The Genesis of the Hashitu Porphyry Molybdenum Deposit, Inner Mongolia, Ne China: Constraints from Mineralogical, Fluid Inclusion, and Multiple Isotope (H, O, S, Mo, Pb) Studies."
Mineralium Deposita 53, no. 3 (Mar 2018): 377-97. http://dx.doi.org/10.1007/s00126-017-0745-5.

plate beneath the Eurasian continental plate, in response to thickening of the crust. Finally, in the Early Cretaceous, there was large-scale crustal delamination and lithospheric thinning.

The I- and A-type granitoids in the Central Asian Orogenic Belt constitute one of the largest plutonic provinces in the world and one of the most important sites of juvenile crust formation during the Phanerozoic (Wu et al., 2011a). Based on their ages of intrusion, these granitoids have been divided in two groups. An early group, with ages of 210 to 275 Ma, is composed mainly of calc-alkaline I- and S-type plutons; the latter were products of post-orogenic extension. Available Sr-Nd isotope data suggest that these magmas were derived from asthenospheric mantle and recycled ancient crust (Chen and Jahn, 2001). The second group, with ages of 130 to 160 Ma, comprises anorogenic A-type plutons associated with lithospheric thinning. These A-type granites were emplaced within NNE to NE trending extensional fault zones and formed from melts derived from the lower crust (Wei et al., 2008).

Numerous ore deposits, including porphyry Cu-Mo, skarn Fe-Sn and polymetallic veins, occur in the southern segment of the GHR Metallogenic Belt (Fig. 2a, Zhai et al. 2014b). Recent exploration has revealed that porphyry Cu-Mo and Mo deposits are particularly common in this area, and has led to the discovery of the Aolunhua, Xiaodonggou, Jiguanshan, Chehugou and Hashitu deposits (Wu et al. 2011b; Zeng et al. 2011; Zhai et al. 2014a). Arguably, one of the most important among them is the Hashitu Mo deposit with reserves of more than 100 Mt of ore and an average grade of 0.13 wt.% Mo. It has been proposed that the magmatic-hydrothermal deposits in this region formed during two different metallogenic events (Li et al., 2012a), an early event in the Late Permian (i.e., 256 ± 7 to 272 ± 3 Ma) and a later event in the Cretaceous and Jurassic (i.e., 129 ± 3 to 167 ± 2 Ma). Most of the porphyry Cu-Mo and Mo deposits formed during the second metallogenic event, which was genetically related to the widespread intrusion of A-type granites (Mao et al. 2005; Liu et al. 2004; Wu et al. 2005, 2011a).

Ore Deposit Geology

The Hashitu Mo deposit is located in the center of the southern segment of the GHR Metallogenic Belt in NE China (Fig. 2a). The main lithotype exposed within the ore district is a composite granitoid, which comprises A-type granite, granite porphyry and NW-trending diorite dikes and sills (Fig. 2b). Field relationships reveal that the granite porphyry intrudes the A-type

Zhai, D. G., J. J. Liu, S. Tombros, and A. E. Williams-Jones. "The Genesis of the Hashitu Porphyry Molybdenum Deposit, Inner Mongolia, Ne China: Constraints from Mineralogical, Fluid Inclusion, and Multiple Isotope (H, O, S, Mo, Pb) Studies." Mineralium Deposita 53, no. 3 (Mar 2018): 377-97. http://dx.doi.org/10.1007/s00126-017-0745-5.

granite as later apophyses (Fig. 2c; Zhai et al. 2014a). The Hashitu granite and porphyry are medium- to coarse-grained, and are composed of equal proportions of quartz and K-feldspar as phenocrysts in a groundmass of quartz, plagioclase, K-feldspar, biotite, muscovite and pyrope, with accessory zircon, fluorite, apatite, titanite, ilmenite and magnetite. Both units are classified as A_2-type granites (Zhai et al., 2014a). They are characterized by high alkali ($K_2O/Na_2O > 1$), fluorine (e.g., occurrence of topaz and fluorite) and Al_2O_3, variable FeO^T and low CaO contents.

Molybdenum mineralization

Five different mineralized sectors make up the Hashitu deposit, namely the South, North, East, Out I and II sectors. These sectors contain more than 100 quartz-molybdenite veins (Fig. 2c) (Lu et al., 2009). The molybdenite ores are mainly vein-type (grading between 0.09 and 7.2 wt.% Mo) but there is also disseminated and stockwork mineralization (grading between 0.08 and 0.36 wt.% Mo, Fig. 3a) (Zhai et al. 2014a). The disseminations and stockworks commonly occur near the main veins in altered granites, but are also observed distal from the vein mineralization. The South zone is the main exploration site and contains more than 60 mineralized veins, most of which are part of the Nº 1 orebody (Fig. 2b). These veins range in thickness from 0.5 to 9 m and have an average thickness of 2 m. They vary in length from 50 to 530 m and their average length is 80 m. The disseminated mineralization occurs mainly in the North zone, particularly in the Nº 4 orebody; the disseminated orebodies are sheet-like, range in thickness from 0.8 to 8.6 m and have an average thickness of 3.5 m.

The Mo-bearing quartz veins occur along the contacts between the granites and the porphyries (Fig. 2c). The Hashitu vein system is developed in the Southern zone and hosts ~90% of the total Mo resource, mainly in 17 large subparallel, NW-trending and steeply dipping Mo-bearing quartz veins (Zhai et al. 2014a). Three distinct sets of quartz veins have been recognized. The earliest is a set of pinkish quartz veins, which was followed, in turn, by sets of smoky quartz and greenish quartz veins. The ore minerals are either disseminated along fractures in the quartz or occur as irregular masses (up to 30 vol. %), which fill fractures or cement quartz fragments in the veins. Pinkish quartz veins (with widths up to 5 m) contain macroscopically euhedral molybdenite (locally up to 25 vol. %), chalcopyrite, galena, sphalerite and pyrite (up to 5 vol. %). Fine- to medium-grained pinkish quartz, muscovite and albite are the main gangue minerals. These veins commonly contain angular granitic fragments. Smoky quartz veins (with widths up to 1 m) consist

Zhai, D. G., J. J. Liu, S. Tombros, and A. E. Williams-Jones. "The Genesis of the Hashitu Porphyry Molybdenum Deposit, Inner Mongolia, Ne China: Constraints from Mineralogical, Fluid Inclusion, and Multiple Isotope (H, O, S, Mo, Pb) Studies." Mineralium Deposita 53, no. 3 (Mar 2018): 377-97. http://dx.doi.org/10.1007/s00126-017-0745-5.

of medium-grained smoky quartz, molybdenite (up to 8 vol. %), rutile, muscovite, chlorite, fluorite, pyrite, marcasite and sphalerite (Fig. 3a-d). The greenish quartz veins, which represent tension-gashes, have widths up to 1.5 m and display well-developed open-space filling textures. Calcite, muscovite, chlorite and epidote usually accompany quartz (Fig. 3f). Sphalerite and pyrite are the main ore minerals (Fig. 3e).

Ore mineralogy and paragenesis

Over thirty ore and gangue minerals have been identified in three primary paragenetic stages (I to III) and a subsequent supergene stage (IV), based on the nature of the mineralization and the mineral assemblages. The early (stages I and II) mineralization is restricted to veins (pink and smokey quartz) and minor stockworks, whereas the late (stage III) mineralization is disseminated and/or occurs as stockworks. Molybdenite comprises more than 90% of the total ore mineral volume, with the remainder comprising minor proportions of pyrite, chalcopyrite, sphalerite, galena, pyrrhotite, and arsenopyrite (Fig. 4a). Stage I is dominated by molybdenite, and is accompanied by subordinate proportions of chalcopyrite, galena, pyrite, arsenopyrite, sphalerite and stannite (Fig. 4b). The molybdenite forms small- to medium-sized isolated platy crystals and is usually associated with quartz, sericite and magnetite (Fig. 3b-d). In the second and main paragenetic stage (stage II), the ore minerals comprise molybdenite, pyrite, sphalerite, chalcopyrite, galena, marcasite and gustavite ($AgPbBi_3S_6$) (Fig. 4c, d), and are accompanied by quartz, hematite, K-feldspar, sericite and locally rutile (Fig. 4e). The Stage II molybdenite normally occurs as massive aggregates, isolated plates or finer disseminations. In the third and final hypogene stage (stage III), pyrite and sphalerite are the main sulfide minerals, and comprise a small proportion of the material; the other minerals are quartz, sericite, dickite and epidote (Fig. 3f). The supergene minerals (stage IV) include molybdite (MoO_3), litharge (PbO) and hematite (Fig. 4f).

Hydrothermal alteration

Widespread silicification affected the Hashitu granites and porphyries. Greisen developed as selvages (with widths of 30 to 50 cm) around joints in which plagioclase (andesine), K-feldspar (orthoclase), biotite and hornblende were replaced by fine-grained muscovite and/or paragonite, chlorite, topaz, fluorite and minor magnetite (Fig. 3a, b). In part, the greisens are spatially related to the disseminated molybdenite mineralization (Fig. 3a).

Greisen selvages are succeeded outwards by texturally destructive, potassic alteration. Potassic

Zhai, D. G., J. J. Liu, S. Tombros, and A. E. Williams-Jones. "The Genesis of the Hashitu Porphyry Molybdenum Deposit, Inner Mongolia, Ne China: Constraints from Mineralogical, Fluid Inclusion, and Multiple Isotope (H, O, S, Mo, Pb) Studies."
Mineralium Deposita 53, no. 3 (Mar 2018): 377-97. http://dx.doi.org/10.1007/s00126-017-0745-5.

assemblages of K-feldspar and muscovite form alteration envelopes surrounding stage I vein-type molybdenite mineralization, and were cut by veins containing stage II mineralization. Muscovite in the potassic zone is commonly associated with sulfides, i.e., molybdenite, pyrite and sphalerite (Fig. 3c, d), and minor albite. Intense to moderately intense argillic alteration zones (with widths up to 30 cm) envelop and are superimposed on the potassic alteration, and grade outward into widespread propylitic alteration. The argillic alteration assemblage is dominated by smoky quartz, dickite and minor paragonite. This type of alteration is pervasive, although primary textures are preserved locally. Clays replaced plagioclase (albite to andesine) and K-feldspar (orthoclase and microcline). The outer propylitic zone (with widths up to 10 cm) is characterized by the assemblage greenish quartz, epidote, fine-grained muscovite and/or paragonite, chlorite, calcite, dolomite, siderite and minor albite and fluorite (Fig. 3f). It occurs predominately along late fractures in the Hashitu granitoids.

Sampling and Analytical Methods

Over sixty samples were collected from the Hashitu Mo deposit, including pinkish, smoky and greenish vein quartz and their associated sulfide minerals (e.g., molybdenite, chalcopyrite and pyrite). Samples were also taken of the Hashitu granites and associated porphyries. Twenty six polished thin sections were examined microscopically and the compositions of their minerals analyzed. The major element compositions of the minerals were determined at the Microprobe Center of the Chinese Academy of Geological Sciences (CAGS), Beijing, China, using a JEOL 8230 Superprobe, equipped with wavelength and energy dispersive detectors and a back-scatter detector. The operating conditions were an acceleration voltage of 15 kV, a beam current of 20 nA and a counting time of 20 s. The beam diameter was set at 1 μm. Natural standards of molybdenite, chalcopyrite, pyrite, sphalerite, galena and synthetic standards of SnO_2, MnTi, and native Ag, Sb, Au, Se, Te and Cd were utilized. ZAF corrections were made with proprietary JEOL software. The detection limit was 0.02 wt% for most elements. The analytical results are reported in Appendix Table 1. Trace element concentrations of sulfide mineral separates (i.e., molybdenite, pyrite and marcasite) and zircon from granite and porphyry were measured using an Agilent 7500a ICP-MS and LA-ICP-MS, respectively, and the results are reported in Appendix Tables 2 and 3. These analyses were carried out at the State Key Laboratory of Geological Processes and Mineral

Zhai, D. G., J. J. Liu, S. Tombros, and A. E. Williams-Jones. "The Genesis of the Hashitu Porphyry Molybdenum Deposit, Inner Mongolia, Ne China: Constraints from Mineralogical, Fluid Inclusion, and Multiple Isotope (H, O, S, Mo, Pb) Studies." Mineralium Deposita 53, no. 3 (Mar 2018): 377-97. http://dx.doi.org/10.1007/s00126-017-0745-5.

211 Resources (GPMR) in the China University of Geosciences, Beijing (CUGB). Details of the
212 analytical method were reported by Zhai et al. (2014a).
213 Hydrogen and oxygen isotopic analyses were conducted on quartz. The analyses were carried out
214 using a MAT-253 stable isotope ratio mass spectrometer at the Beijing Research Institute of Uranium
215 Geology, China National Nuclear Corporation (CNNC). Oxygen was released from the quartz using
216 the BrF_5 extraction technique and hydrogen was released from fluid inclusions in quartz grains by
217 thermal decrepitation. The analytical precision was better than ± 0.2 ‰ for $\delta^{18}O$ and ± 2 ‰ for δD.
218 The isotopic ratios are reported in standard δ notation (‰) relative to SMOW for oxygen and
219 hydrogen (Table 1).
220 Samples of common sulfides (i.e., molybdenite, pyrite, chalcopyrite, pyrrhotite and galena) were
221 obtained for conventional sulfur isotope analyses by drilling sulfide-bearing ores and thin sections
222 using a 0.3 mm carbide bit under an optical microscope. Prior to micro-drilling, all the minerals in the
223 samples were checked under a transmitted light microscope in order to confirm that the grains of the
224 different minerals are in apparent textural equilibrium (Fig. 5). The samples were analyzed using a
225 Finnigan MAT-252 stable isotope ratio mass spectrometer at the Department of Geological Sciences,
226 Indiana University, Bloomington, USA. The standard V_2O_5-SO_2 method was utilized for the
227 analyses following the procedures outlined by Lefticariu et al. (2006). The sulfur isotopic ratios are
228 reported in standard δ notation ‰ relative to V-CDT. Analytical precision was better than ± 0.05 ‰
229 and the reproducibility was within ±0.2‰ (± 2σ). The sulfur isotopic ratios are listed in Table 2.
230 The molybdenum isotopic composition of molybdenite was determined using a MC-ICP-MS,
231 Neptune®, Thermo Finnigan at BRGM, Orléans, France, following the methods of Arnold et al.
232 (2004) and Pietruszka et al. (2006). In order to maximize precision, all samples were analyzed at
233 least three times in different sequences and the average value was used for subsequent data
234 interpretation. Values of $\delta^{98/95}Mo$ and $\delta^{97/95}Mo$ were evaluated using the equations of Pietruszka et
235 al. (2006) and are reported as ‰. All data are reported at the ± 2σ level relative to NIST SRM 3134
236 with an external reproducibility of 0.09‰ and 0.06‰ for $\delta^{98/95}Mo$ and $\delta^{97/95}Mo$, respectively. The
237 Mo isotopic data are listed in Table 3.
238 The Pb isotopic compositions of the sulfides were determined at the Chinese Academy of
239 Geological Sciences (CAGS), Beijing, China. The analyses were carried out using an England Nu
240 Plasma High Resolution type MC-ICP-MS with standard NBS 981. Long-term repeated

Zhai, D. G., J. J. Liu, S. Tombros, and A. E. Williams-Jones. "The Genesis of the Hashitu Porphyry Molybdenum Deposit, Inner Mongolia, Ne China: Constraints from Mineralogical, Fluid Inclusion, and Multiple Isotope (H, O, S, Mo, Pb) Studies." Mineralium Deposita 53, no. 3 (Mar 2018): 377-97. http://dx.doi.org/10.1007/s00126-017-0745-5.

measurement of lead isotopic ratios of standard NBS 981 yielded a $^{208}Pb/^{206}Pb$ value of 2.1674 ± 0.0005, a $^{207}Pb/^{206}Pb$ value of 0.91486 ± 0.00025, a $^{206}Pb/^{204}Pb$ value of 16.9397 ± 0.0111, a $^{207}Pb/^{204}Pb$ value of 15.4974 ± 0.0089, and a $^{208}Pb/^{204}Pb$ value of 36.7147 ± 0.0262 (± 2σ). The lead isotopic data are reported in Table 4.

Microthermometric measurements were performed on fluid inclusions in quartz from Mo-bearing quartz veins and quartz phenocrysts from the mineralized granitoids. The microthermometric data were obtained using a LINKAM MDSG600 heating-freezing stage coupled to a ZEISS microscope at the School of Earth Sciences and Resources, China University of Geosciences Beijing (CUGB). The stage enables measurements within the range of -196° to 600°C. A high temperature MDSG600 heating-freezing stage was utilized for melt inclusion measurements. This instrument has a temperature range from 25° to 1200°C. The microthermometric results are reported in Table 5. Single fluid inclusion laser Raman spectroscopic analysis was carried out at the Beijing Research Institute of Uranium Geology, China National Nuclear Corporation (CNNC), using a Renishaw RM-2000 Raman spectroscopic microscope. This instrument records peaks in the range of 100 to 4000 cm^{-1} with a resolution of 1 to 2 cm^{-1}. The spot size of the laser beam is about 1 μm. The inclusions were analyzed for CO_2, CH_4, N_2, CO, H_2S, SO_2, C_2H_6, NH_3 and H_2, and the most common monoatomic and polyatomic ions and molecules.

Results

Mineral chemistry

The results of microprobe analyses show that the Mo/S ratio of molybdenite is 1.42 and 1.45 in stages I and II, respectively (Appendix Table 1), reflecting differential incorporation of Cu, Bi and Cd into this mineral. Stage II arsenopyrite is characterized by a X_{As} % of 29.93. The stannite (Stage II) has a $\log X_{FeS}/X_{ZnS}$ value of -0.13 and the sphalerite contains 7.66 wt % Fe (X_{FeS} = 15.8 % and $\log X_{FeS}/X_{ZnS}$ of -0.82). The chondrite-normalized REE and primitive mantle-normalized trace element profiles of the ore minerals, i.e., molybdenite, pyrite and marcasite, and the host granitic rocks are very similar (Fig. 6). Both sets of profiles (sulfides, Hashitu granites and porphyries) display negative Eu anomalies and weak LREE enrichment (Appendix Table 2, Fig. 6a, c), whereas the zircon from granite and porphyry shows HREE enrichment with a negative Eu anomaly (Appendix Table 3, Fig. 6e, f); molybdenite exhibits a peaks for Sm. On a primitive mantle-normalized spidergram, both granites and porphyries generally display positive Pb, Nb, Sm,

Zhai, D. G., J. J. Liu, S. Tombros, and A. E. Williams-Jones. "The Genesis of the Hashitu Porphyry Molybdenum Deposit, Inner Mongolia, Ne China: Constraints from Mineralogical, Fluid Inclusion, and Multiple Isotope (H, O, S, Mo, Pb) Studies."
Mineralium Deposita 53, no. 3 (Mar 2018): 377-97. http://dx.doi.org/10.1007/s00126-017-0745-5.

U and Th anomalies and negative Ba, Sr, Zr and Ta anomalies (Fig. 6b, d). The sulfide minerals have Rb/Nb, Ta/Nb, Th/U and Zr/Sr ratios of up to 9.1, and 10.5, 0.1 and < 6.4, compared to the values of > 12.5, > 0.1 and < 1 and 10 that are typical of molybdenite in "Climax-type" molybdenum deposits (Wallace, 1995). The sulfide mineral ratios are almost identical to those for the associated granites and porphyries (Zhai et al., 2014a).

Isotope geochemistry

Hydrogen and oxygen isotope compositions

Hydrogen and oxygen isotope compositions were obtained from pinkish, smoky and greenish quartz in veins containing sulfides. The δD_{H2O} values display a narrow range, i.e., from -105.8 to -87.3‰; whereas the $\delta^{18}O_{SMOW}$ values display a relatively large range, i.e., from +9.3 to +15.7‰ (Table 1). Quartz from Stage I and II veins is commonly characterized by high δD_{H2O} and $\delta^{18}O_{SMOW}$ values relative to quartz in stage III veins.

Sulfur isotope compositions

Overall, the $\delta^{34}S_{V\text{-}CDT}$ values range from +0.4 to +3.8‰ with an average of +2.4‰ (Table 2). The $\delta^{34}S$ values of molybdenite and chalcopyrite are very similar; they both average 2.49‰, and range from 1.69 to 3.80‰ (n=5) and 1.66 to 3.09‰ (n=10), respectively. In comparison, the values for pyrite show a relatively large variation, ranging from 0.40 to 3.54‰ (n=26) with an average of 2.34‰. A single analysis of pyrrhotite yielded a $\delta^{34}S$ value of 2.30‰ and two analyses of galena yielded $\delta^{34}S$ values of 2.54 and 2.88‰.

Molybdenum isotopes

Molybdenum isotope compositions were obtained from stage I and II molybdenite (Table 3). In general, stage I molybdenite displays lower molybdenum isotope values than stage II molybdenite. The $\delta^{98/95}Mo$ and $\delta^{97/95}Mo$ values range from 0 to +0.37‰ and 0 to +0.26‰, respectively. All of the $\delta^{98/95}Mo$ and $\delta^{97/95}Mo$ ratios correlate linearly (r^2 = 0.995) (Fig. 7), suggesting that isobaric interferences were largely eliminated and appropriate adjustments were applied to correct for analytically induced mass fractionation. In addition, the fact that the variations of $\delta^{97/95}Mo$ and $\delta^{98/95}Mo$ are very similar indicates that the measured Mo isotopic ratios were almost entirely the product of natural mass-dependent fractionation. This is supported by the observation that intra-sample variations of up to 0.14‰ and 0.19‰ for $\delta^{97/95}Mo$ and $\delta^{98/95}Mo$, respectively, were determined for individual molybdenite crystals within the same hand specimen

Zhai, D. G., J. J. Liu, S. Tombros, and A. E. Williams-Jones. "The Genesis of the Hashitu Porphyry Molybdenum Deposit, Inner Mongolia, Ne China: Constraints from Mineralogical, Fluid Inclusion, and Multiple Isotope (H, O, S, Mo, Pb) Studies." Mineralium Deposita 53, no. 3 (Mar 2018): 377-97. http://dx.doi.org/10.1007/s00126-017-0745-5.

(e.g., sample HST-20a and b, Table 3).

Lead isotope compositions

Lead isotope compositions were determined for molybdenite, pyrite and pyrrhotite. The measured $^{206}Pb/^{204}Pb$, $^{207}Pb/^{204}Pb$ and $^{208}Pb/^{204}Pb$ ratios are listed in Table 4. In general, molybdenite is characterized by higher lead isotope ratios than pyrite and pyrrhotite. The $^{206}Pb/^{204}Pb$ and $^{208}Pb/^{204}Pb$ ratios for pyrite range from 18.3256 to 18.8958 (the average is 18.6450), and 38.1808 to 42.9744 (the average is 39.4557), respectively. The pyrrhotite $^{206}Pb/^{204}Pb$ and $^{208}Pb/^{204}Pb$ ratios are similar, i.e., 18.2579 to 18.2671 and 38.0984 to 38.1084, respectively. Moreover, there is no evident variation in the ratios of different textural types of molybdenite, pyrite or pyrrhotite (Table 4).

Fluid and melt inclusions

Fluid inclusions

Fluid inclusions were analyzed microthermometrically in quartz from the different vein stages (i.e., the pinkish, smoky and greenish quartz veins) and quartz phenocrysts from granites and porphyries. Only fluid inclusions deemed to be primary from their occurrence in 3-D clusters or along growth zones were analyzed, and each cluster or set of inclusions along a growth zone was considered to represent a separate fluid inclusion assemblage (FIA). The inclusions in the clusters and along growth zones are elliptical, rod-shaped, rounded, irregular or display negative crystal shapes, and range in length from 10 to 30 μm (Fig 8). Fluid inclusions, which occur along fractures or grain boundaries in clusters and linear arrays, were considered secondary and were not analyzed microthermometrically.

Fluid inclusions were classified on the basis of the phase relationships observed at room temperature (Fig 8). Four types of fluid inclusions were recognized: (i) aqueous liquid and vapor inclusions (L-V, Fig. 8a), which homogenize to liquid upon heating (they generally contain ~ 60 to 80 vol. % liquid); (ii) vapor-rich aqueous inclusions (V-L, Fig. 8b), which homogenize to vapor (they typically contain > 60 vol. % vapor); (iii) monophase vapor or liquid aqueous inclusions (type V or L, Fig. 8c); and (iv) solid-bearing aqueous liquid-vapor inclusions (L-V-S, Fig. 8d-g) with 20 to 65 vol. % vapor. Laser-Raman analyses of individual fluid inclusions indicate that the vapor was dominated by H_2O but also contains CO_2 (Fig. 9a, b). Raman spectra for the liquid indicate that

Zhai, D. G., J. J. Liu, S. Tombros, and A. E. Williams-Jones. "The Genesis of the Hashitu Porphyry Molybdenum Deposit, Inner Mongolia, Ne China: Constraints from Mineralogical, Fluid Inclusion, and Multiple Isotope (H, O, S, Mo, Pb) Studies." Mineralium Deposita 53, no. 3 (Mar 2018): 377-97. http://dx.doi.org/10.1007/s00126-017-0745-5.

331 CO_2(aq) and SO_4^{2-} are the principal dissolved aqueous species in addition to Cl^-, which was
332 analyzed microthermometrically (Fig. 9c, d). No CO_2-rich fluid inclusions were observed, although
333 Raman analyses showed that CO_2 is present in both the liquid and the vapor. Based on its cubic
334 shape, halite was identified to be the principal solid (Fig. 8d, e); hematite, calcite and rhodochrosite
335 were identified from their color, in the case of hematite (Fig. 8f, i), and Raman spectra (Fig. 9e, f).
336 All except the monophase inclusions are commonly observed (Fig. 8d, e). The common coexistence
337 of L-V, V-L, L-V-S and monophase inclusions along the same growth zone of single quartz crystals
338 provides evidence that the fluid underwent phase separation (Fig. 8d-f, i). It also suggests that,
339 except for halite, the solids were trapped phases; halite-bearing L-V-S inclusions did not coexist
340 with L-V inclusions.
341 Microthermometric measurements were performed on L-V, V-L and L-V-S inclusions. Most L-V
342 inclusions and the liquid and vapor in L-V-S inclusions homogenized to liquid and V-L inclusions
343 homogenized to vapor. Homogenization temperatures were determined for 275 fluid inclusions,
344 including approximately 25 FIAs, and final ice melting temperatures were determined for a subset
345 of 22 of these FIAs (Fig. 10, Table 5). The homogenization temperatures of type L-V, and V-L
346 inclusions range from ~ 91° to 596°C (average of 302ºC), and 300° to 591°C (average of 454ºC).
347 Most L-V-S inclusions did not homogenize because of the failure of one of the solids to dissolve.
348 However, the liquid and vapor phases in these inclusions homogenized at temperatures between
349 160° and 600°C (average of 372ºC), respectively (Fig. 10a). The halite in L-V-S inclusions
350 containing this mineral dissolved at temperatures between 190 and 553 ºC. Fluid inclusion
351 assemblages in stage I, II and III veins have average homogenization temperatures of 385ºC, 325ºC
352 and 285ºC, respectively.
353 The average final ice melting temperature (T_m) for type L-V inclusions in individual FIAs
354 ranged from -22 to -0.4 ºC (Table 5), corresponding to a salinity range from 0.7 to 23.7 wt% NaCl
355 equivalent (salinity was estimated from the equations of Brown and Lamb 1989) (Fig. 10b). Halite
356 dissolution temperatures were utilized to calculate the salinity of halite-bearing L-V-S inclusions
357 (calculations were based on Lecumberri-Sanchez et al., 2012). As noted above, this temperature
358 ranged from 190° to 553°C. Halite dissolution of L-V-S inclusions occurred at lower temperature
359 than L-V homogenization. The corresponding range in salinity is from 31.4 to 65.5 wt% NaCl
360 equivalent (Fig. 10b). The different FIA types show distinct temperature and salinity ranges (Fig.

Zhai, D. G., J. J. Liu, S. Tombros, and A. E. Williams-Jones. "The Genesis of the Hashitu Porphyry Molybdenum Deposit, Inner Mongolia, Ne China: Constraints from Mineralogical, Fluid Inclusion, and Multiple Isotope (H, O, S, Mo, Pb) Studies."
Mineralium Deposita 53, no. 3 (Mar 2018): 377-97. http://dx.doi.org/10.1007/s00126-017-0745-5.

10c), i.e., halite-bearing L-V-S dominant FIAs have relatively high salinity and homogenization temperatures, which overlap part of the temperature range for the L-V dominant and V-L dominant FIAs, whereas the latter two FIA types exhibit much lower ranges in salinity.

Melt inclusions

Melt inclusions were identified in quartz phenocrysts from the granites and porphyries. The melt inclusions (up to 20 μm) usually contain glass, liquid and vapor (Fig. 8h). Most melt inclusions homogenized to a silicate liquid at temperatures varying from ~ 640° to 860°C (Fig. 10a). These temperatures are broadly consistent with the crystallization temperatures estimated for the Hashitu granitic magmas based on the Ti-in-zircon geothermometer (Watson et al., 2006), of ~ 583° to 760°C.

Discussion

Temperature-pressure conditions

The temperature of Mo mineralization at Hashitu was estimated using a combination of fluid inclusion and stable isotope geothermometers. Microthermometric measurements of fluid inclusion assemblages hosted in stages I, II and III quartz veins yield average homogenization temperatures (Th) of 385ºC, 325ºC and 285ºC, respectively. As L-V or halite-bearing L-V-S inclusions coexisted with V-L inclusions in the same FIAs, the fluid is interpreted to have boiled (or condensed) and these temperatures represent the temperatures of entrapment. Similar temperatures were obtained using the pyrite-chalcopyrite, pyrite-galena, chalcopyrite-galena and molybdenite-chalcopyrite isotope geothermometers, i.e., from 384° to 434°C and 304° to 318°C for stages I and II, respectively (calculated using the equations of Ohmoto and Rye, 1979). The pressure during the different mineralizing stages was calculated using the 'HOKIE FLINCS_H2O-NACL' spreadsheet for a boiling fluid system (Steele-MacInnis et al., 2012). These calculations indicate that stage I quartz veins were trapped at pressures of 300 to 610 bars (440 bars on average), which correspond to depths of 1.5 to 2.4 km, assuming lithostatic conditions or X to Y km, assuming hydrostatic conditions. The corresponding pressures for stages II and III quartz veins range from 80 to 230 bars (130 bars on average) and 50 to 90 bars (75 bars on average), respectively.

Based on the data from fluid inclusion microthermometry and stable isotope geothermometry, we conclude that main stage molybdenite deposition (stage II) in the Hashitu deposit occurred at

Zhai, D. G., J. J. Liu, S. Tombros, and A. E. Williams-Jones. "The Genesis of the Hashitu Porphyry Molybdenum Deposit, Inner Mongolia, Ne China: Constraints from Mineralogical, Fluid Inclusion, and Multiple Isotope (H, O, S, Mo, Pb) Studies."
Mineralium Deposita 53, no. 3 (Mar 2018): 377-97. http://dx.doi.org/10.1007/s00126-017-0745-5.

391 temperatures between 285º and 325°C and near hydrostatic pressures of 80 to 230 bars. Overall, the
392 data presented above indicate that vein formation in the Hashitu Mo deposit occurred at
393 progressively lower pressure and lower temperature.
394
395 ***Other physicochemical conditions***
396 Physicochemical conditions, other than pressure and temperature, during the formation of ore
397 and alteration minerals were estimated from stability relationships among sulfides and silicates
398 using the SUPCRT92 database (Johnson et al., 1992). As discussed above, mineralization stages I,
399 II and III are estimated to have occurred at temperatures of 385°, 325° and 285°C and pressures of
400 440, 130 and 75 bars, respectively. For the purpose of estimating stability relationships among the
401 minerals, all were considered to be ideal solid solutions.
402 From the alteration mineral assemblages, K-feldspar-muscovite-albite (stage II), and muscovite-
403 dickite- paragonite (stage III), the $\log(\alpha K^+/\alpha H^+)$ is estimated to have been 3.64 and 1.76, and the
404 $\log(\alpha Na^+/\alpha H^+)$ 4.54 and 3.43, respectively, assuming temperatures for stages II and III of 325º and
405 285 ºC (Fig. 11). During the transition from potassic to argillic alteration, the ore fluids evolved by
406 decreasing both $\log(\alpha K^+/\alpha H^+)$ and $\log(\alpha Na^+/\alpha H^+)$, which resulted in the destruction of K-feldspar
407 and the stabilization of dickite in stage III. To constrain fO_2 conditions for the main ore stage (stage
408 II), a logfO_2–pH diagram was constructed utilizing aqueous and mineral equilibria in the Fe–O–S
409 system, assuming a temperature of 325°C and a pressure of 0.13 kbars (Fig. 12). The alteration
410 minerals associated with the sulfides in stage II were used to constrain the pH. Thermodynamic
411 data for the calculations were taken from Johnson et al. (1992), Robie and Hemingway (1995), and
412 Pal'yanova and Drebushchak (2002). As formation of the main ore-stage veins involved
413 precipitation of pyrite, chalcopyrite, muscovite and K-feldspar (Fig. 3), we conclude, based on
414 Figure 12, that the conditions of the main stage of ore deposition were relatively oxidizing ($\Delta\log$
415 fO_2 (HM) = +1.5) and weakly acidic (pH=5.6).
416
417 ***Source of metallic and hydrothermal components of the ore fluids***
418 The calculated $\delta^{34}S_{H2S}$ values of the mineralizing fluid interpreted to have been in equilibrium
419 with the sulfide minerals range between +0.3 and +3.9‰ (Table 2, Fig. 13b), which is consistent
420 with a magmatic origin for the ore fluid, e.g., the local Hashitu granitic magma. It is also

Zhai, D. G., J. J. Liu, S. Tombros, and A. E. Williams-Jones. "The Genesis of the Hashitu Porphyry Molybdenum Deposit, Inner Mongolia, Ne China: Constraints from Mineralogical, Fluid Inclusion, and Multiple Isotope (H, O, S, Mo, Pb) Studies." Mineralium Deposita 53, no. 3 (Mar 2018): 377-97. http://dx.doi.org/10.1007/s00126-017-0745-5.

421 noteworthy that sulfur isotope values varied during sulfide mineral crystallization as shown by the
422 variation of $\delta^{34}S_{H2S}$ on a millimetric scale in single crystals (Fig. 5), which may indicate minor
423 variations in log fO_2 – pH conditions (Fig. 12).

424 The measured $\delta^{98/95}$Mo and $\delta^{97/95}$Mo compositions of the molybdenite, which are similar to those
425 of the granites (Anbar et al., 2001), suggest that the most likely source of molybdenum was the
426 genetically associated granitic magma. A positive correlation between the molybdenum and sulfur
427 isotope values of the Hashitu molybdenite is evident from plots of $\delta^{34}S_{V\text{-}CDT}$ versus $\delta^{98/95}Mo_{NIST}$
428 and $\delta^{97/95}Mo_{NIST}$ (Fig. 13c, d). These plots indicate that the heavier Mo isotope is associated with
429 the heavier S isotope (r^2 = 0.92, Fig. 13c-d), and suggest reduction of the fluid during molybdenite
430 precipitation; high δ^{34}S values can be explained by a reduction in fO_2 (Fig. 12). Such an
431 interpretation is consistent with the observation that in hydrothermal fluids Mo is generally
432 transported in the hexavalent state but precipitates in the tetravalent state as the mineral
433 molybdenite (Williams-Jones and Migdisov, 2014). During this reduction, heavy Mo isotopes will
434 be partitioned preferentially into molybdenite (Tossel 2005; Greber et al., 2013). It should be noted
435 that two samples have values lying off the linear trend referred to above (Fig. 13c-d). We infer that
436 these anomalous values likely indicate disequilibrium during the formation of the corresponding
437 molybdenite. This is consistent with the observed Mo and S isotope variations on a millimetric
438 scale in hand specimens, which mostly reflect fO_2 fluctuations due to boiling (or condensation).

439 In order to further evaluate the metal source, we made use of previously published Pb isotopic
440 data, including Pb isotope ratios for local Permian, Jurassic and Cretaceous volcanosedimentary
441 rocks and granitoids, and Pb isotope data for nearby hydrothermal ore deposits (i.e., the
442 Huangganglang Fe-Sn deposit) (Fig. 14a, b). A considerable body of lead isotope data was also
443 collected for the Linxi A-type pluton, which is located near the Hashitu granite (~ 20 km from it)
444 and is similar in age and composition to the latter. Based on the distribution of $^{206}Pb/^{204}Pb$,
445 $^{207}Pb/^{204}Pb$ and $^{208}Pb/^{204}Pb$ ratios in binary plots of these ratios, the most likely source of Pb in the
446 Hashitu sulfides is the upper crust. There may also be a minor mantle contribution (Fig. 14). The Pb
447 isotopic ratios of the Mesozoic granitic rocks are linearly distributed on these plots, implying a
448 variable source region. Significantly, the Pb isotopic ratios of the ore minerals (i.e., molybdenite,
449 pyrite and pyrrhotite) are intermediate between those of the Mesozoic granites, with which the Mo
450 deposit is closely associated, and the Jurassic volcanic rocks, which underlie both the Mo deposit

Zhai, D. G., J. J. Liu, S. Tombros, and A. E. Williams-Jones. "The Genesis of the Hashitu Porphyry Molybdenum Deposit, Inner Mongolia, Ne China: Constraints from Mineralogical, Fluid Inclusion, and Multiple Isotope (H, O, S, Mo, Pb) Studies."
Mineralium Deposita 53, no. 3 (Mar 2018): 377-97. http://dx.doi.org/10.1007/s00126-017-0745-5.

451 and the intrusion. This suggests that there were contributions of Pb and possibly other metals from
452 both sources.

453 The $\delta^{18}O_{H2O}$ values calculated from the corresponding values for quartz and the interpreted
454 trapping temperatures of the fluid have a relatively large range, i.e., from +1.85 to +9.65‰;
455 whereas the measured δD_{H2O} values have a relatively narrow range, i.e., from -105.8 to -87.3‰
456 (Table 1). The $\delta^{18}O_{H2O}$ values for stage I and II veins are similar to those of magmatic water,
457 whereas those for stage III are lower. By contrast, the δD_{H2O} values for all stages plot below the
458 field for magmatic water (Fig. 13a). We attribute the latter to a bulk fluid dominated by secondary
459 inclusions of meteoric composition and therefore conclude, on the basis of the $\delta^{18}O_{H2O}$ data, that
460 the stage I and II veins crystallized from magmatic fluids and the stage III fluids from an evolved
461 meteoric fluid.

462

463 ***Hydrothermal Fluid Evolution***

464 The Hashitu Mo deposit is genetically related to an A-type granite, which exsolved a
465 magmatic hydrothermal fluid that was responsible for Mo mineralization and hydrothermally
466 altered the rock. Temperature during the early porphyry stage was between ~640° to 760°C, based
467 on the application of the Ti-in-zircon geothermometer (Appendix Table 3). Pressure is interpreted
468 to have been in the range of 300 to 600 bars based on the homogenization temperature of a boiling
469 (or condensing) set of fluid inclusion assemblages. These pressures correspond to depths of 1.5 to
470 2.4 km. At this depth and pressure, the exsolved fluids were initially of low to intermediate salinity
471 but evolved to an assemblage of high salinity L-V-S and/or L-V fluids and low salinity V-L fluids
472 through boiling/condensation induced by a transition from lithostatic to hydrostatic pressure (Fig.
473 10c). Temperature during the emplacement of the magmatic fluid-dominated stage I and II veins
474 was ~385ºC and ~325ºC, respectively, but decreased to ~285 ºC during the transition to a meteoric
475 fluid dominated system.

476

477 ***Metal transport and deposition***

478 The fluid inclusion and isotopic data presented earlier demonstrate convincingly that the fluid
479 responsible for Mo mineralization at Hashitu was exsolved from a magma, which was also the
480 source of the metals. Given the relatively shallow level of emplacement of the hydrothermal system

Zhai, D. G., J. J. Liu, S. Tombros, and A. E. Williams-Jones. "The Genesis of the Hashitu Porphyry Molybdenum Deposit, Inner Mongolia, Ne China: Constraints from Mineralogical, Fluid Inclusion, and Multiple Isotope (H, O, S, Mo, Pb) Studies." Mineralium Deposita 53, no. 3 (Mar 2018): 377-97. http://dx.doi.org/10.1007/s00126-017-0745-5.

(between 1.5 and 2.4 km), the exsolved fluid was likely of low to intermediate density (Williams-Jones and Migdisov, 2014). In order to determine its density prior to further phase separation, we assumed that the fluid had a salinity of ~10 wt. % NaCl equivalent (Burnham, 1979), a temperature of ~750 ºC (the likely emplacement temperature of the magma) and an emplacement pressure of ~500 bars (lithostatic pressure). Based on these data, the fluid had a density of ~0.17 g/cm^{-3}, indicating that it exsolved as a vapor-like supercritical fluid and, on cooling, condensed a high salinity liquid.

Although there has been some debate over the capacity of low density fluids to transport (see Williams-Jones and Heinrich, 2005), the recent experimental studies of Migdisov and Williams-Jones (2013), Migdisov et al., (2014), and Hurtig and Williams-Jones (2014 a and b) have resolved this issue, showing that Ag, Cu, Au and Mo can all be transported in appreciable concentrations by vapor. In the case of Mo, an oxidizing vapor-like fluid (low concentrations of reduced sulfur species) of the density inferred above would be capable of transporting 100s of ppm Mo at near magmatic conditions as the Mo(VI) species ($MoO_3(H_2O)_y$), i.e., more than sufficient to form an ore deposit (Hurtig and Williams-Jones, 2015). Furthermore, the modeling conducted in this paper and in Hurtig and Williams-Jones (2014b) showed convincingly that molybdenum solubility decreases with decreasing temperature and particularly decreasing oxygen fugacity, which ultimately reduces Mo(VI) to Mo(IV) and sulfate to H_2S, thereby causing deposition of molybdenite (see also Williams-Jones and Migdisov, 2014). This behavior of molybdenum is consistent with the fluid evolution of the Hashitu system described above, in which temperature decreased from the early to late stage veins and fO_2 was relatively high (as shown by the presence of hematite) and decreased in absolute terms with decreasing temperature. It is, however, important to recall that the Mo mineralization coincided with a decrease in pressure, which induced condensation of the vapor and that the latter likely also played a role in molybdenite deposition by sharply reducing ligand activity and hydration, and further decreasing temperature (Seward et al., 2014; Williams-Jones and Migdisov, 2014). Accordingly, we propose that that shallow emplacement of an A-type granite, exsolution of a low density magmatic ore fluid and a combination of decreasing temperature, fO_2 and pressure all contributed to ore formation at Hashitu.

Zhai, D. G., J. J. Liu, S. Tombros, and A. E. Williams-Jones. "The Genesis of the Hashitu Porphyry Molybdenum Deposit, Inner Mongolia, Ne China: Constraints from Mineralogical, Fluid Inclusion, and Multiple Isotope (H, O, S, Mo, Pb) Studies."
Mineralium Deposita 53, no. 3 (Mar 2018): 377-97. http://dx.doi.org/10.1007/s00126-017-0745-5.

Comparisons between Hashitu and other Climax type Mo deposits

The Hashitu Mo deposit displays numerous features that are common to those of Climax Mo deposits, e.g., ore shells of quartz-molybdenite stockwork veins that lie above and surround the greisen-altered apices of highly evolved calc-alkaline A-type granites. As noted previously, Climax-type porphyry molybdenum deposits are extremely rare and only thirteen deposits, all occurring in western North America with ages ranging from Late Cretaceous to mainly Tertiary, have been descried in the literature (Ludington and Plumlee, 2009). These deposits all have a post-subduction and extensional tectonic setting. By contrast, the newly discovered Hashitu Mo deposit in NE China was formed in association with late-Jurassic granitic plutons in a distal back arc, syn-subduction setting (basin-and-range) (Zhai et al., 2014a). The discovery of the Hashitu Mo deposit indicates that Climax-type Mo deposits could also form during subduction instead of post-subduction as previously suggested. Owing to the different tectonic history of western North America and NE China, Mo deposits in the latter region show notable differences from established Climax-type deposits. However, recognition of the existence of these deposits in NE China provides an important opportunity to gain new insights into the genesis of Climax-type deposits generally, and to explore efficiently for the Hashitu variant in other parts of the World.

Conclusions

Geological, mineralogical, fluid inclusion and multiple isotope investigations of the newly-discovered Hashitu Mo deposit provide compelling evidence that both ore-forming fluids and metallic ions were genetically related to a felsic magma, which was emplaced at shallow crustal levels in response to oceanic subduction in NE China. Hydrothermal fluids exsolved from the evolved magma were initially supercritical, saline, acid, oxidizing and of low density, and unmixed into high salinity LVS and low salinity LV and VL fluids. A model is proposed in which low density hydrothermal fluids released from an oxidising A-type magma transported Mo as hydrated MoO_3 species and deposited large masses of molybdenite in response to a combination of decreasing temperature, decreasing oxygen fugacity and condensation (which decreased ligand activity , hydration and temperature). The Hashitu Mo deposit shows similarities to and differences from typical Climax Mo deposits, which may be helpful in understanding the genesis of porphyry Mo deposits in various tectonic settings.

Zhai, D. G., J. J. Liu, S. Tombros, and A. E. Williams-Jones. "The Genesis of the Hashitu Porphyry Molybdenum Deposit, Inner Mongolia, Ne China: Constraints from Mineralogical, Fluid Inclusion, and Multiple Isotope (H, O, S, Mo, Pb) Studies."
Mineralium Deposita 53, no. 3 (Mar 2018): 377-97. http://dx.doi.org/10.1007/s00126-017-0745-5.

Acknowledgement

This research was supported financially by the National Natural Science Foundation of China (Grant 41503042), the Fundamental Research Funds for the Central Universities (Grant 2652015045), the Open Research Funds for GPMR (Grant GPMR201513) and the Chinese "111" project (Grant B07011). We thank Ed Ripley and Ben Underwood for the sulfur isotope analyses, and Noémie Breillat for the molybdenum isotope analyses. Xingwang Liu and Gongwen Wang helped with the field work and Wenbing Zhu with the preparation of samples for H-O isotope analyses. Discussions with and helpful suggestions from Chusi Li considerably helped us to clarify some of the ideas presented in the manuscript. An initial draft of the manuscript was prepared during the visit of DZ to Indiana University in 2013-2014, which was funded by the China Scholarship Council.

References

Zhai, D. G., J. J. Liu, S. Tombros, and A. E. Williams-Jones. "The Genesis of the Hashitu Porphyry Molybdenum Deposit, Inner Mongolia, Ne China: Constraints from Mineralogical, Fluid Inclusion, and Multiple Isotope (H, O, S, Mo, Pb) Studies." Mineralium Deposita 53, no. 3 (Mar 2018): 377-97. http://dx.doi.org/10.1007/s00126-017-0745-5.

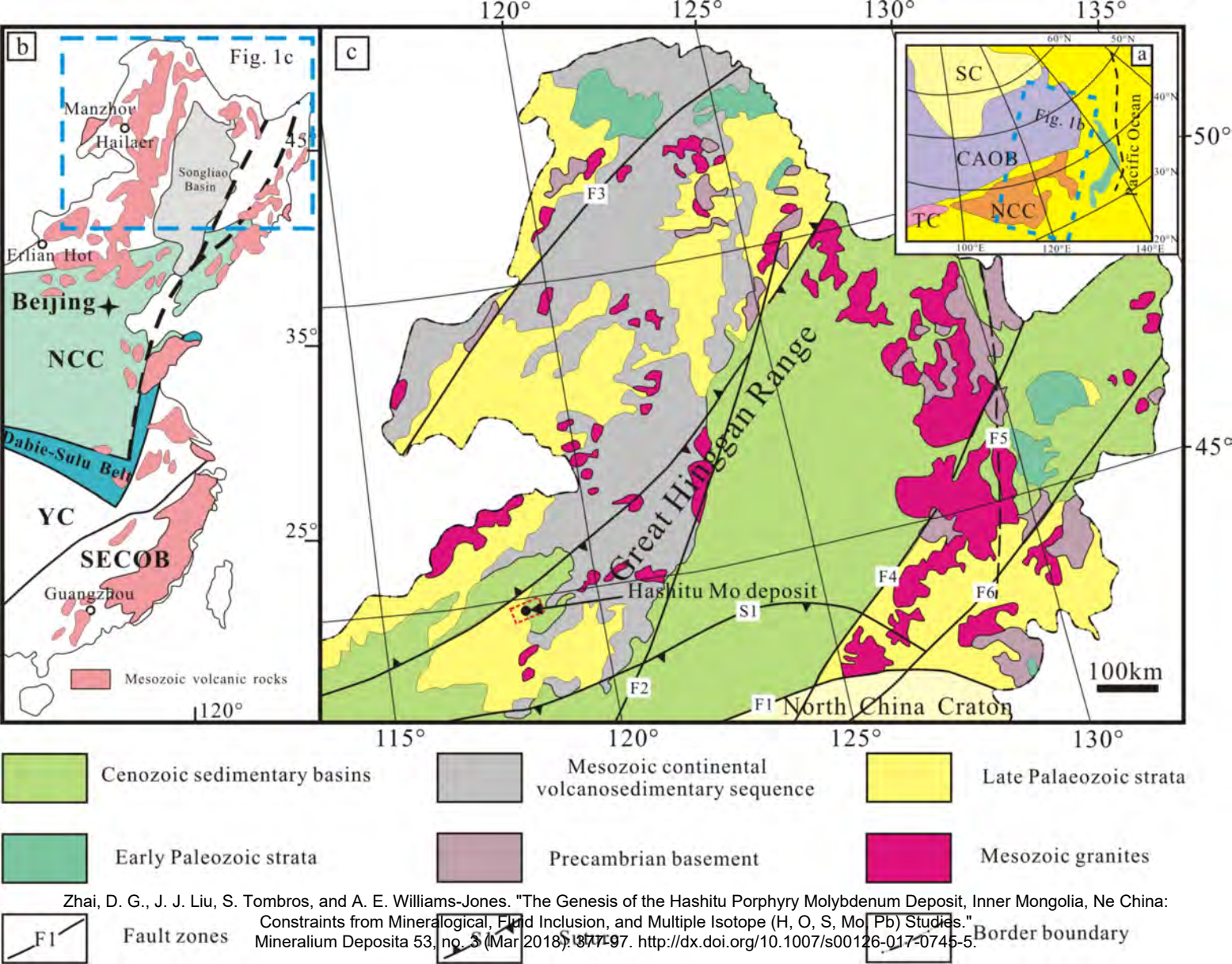

Zhai, D. G., J. J. Liu, S. Tombros, and A. E. Williams-Jones. "The Genesis of the Hashitu Porphyry Molybdenum Deposit, Inner Mongolia, Ne China: Constraints from Mineralogical, Fluid Inclusion, and Multiple Isotope (H, O, S, Mo, Pb) Studies." Mineralium Deposita 53, no. 3 (Mar 2018): 377-97. http://dx.doi.org/10.1007/s00126-017-0745-5.

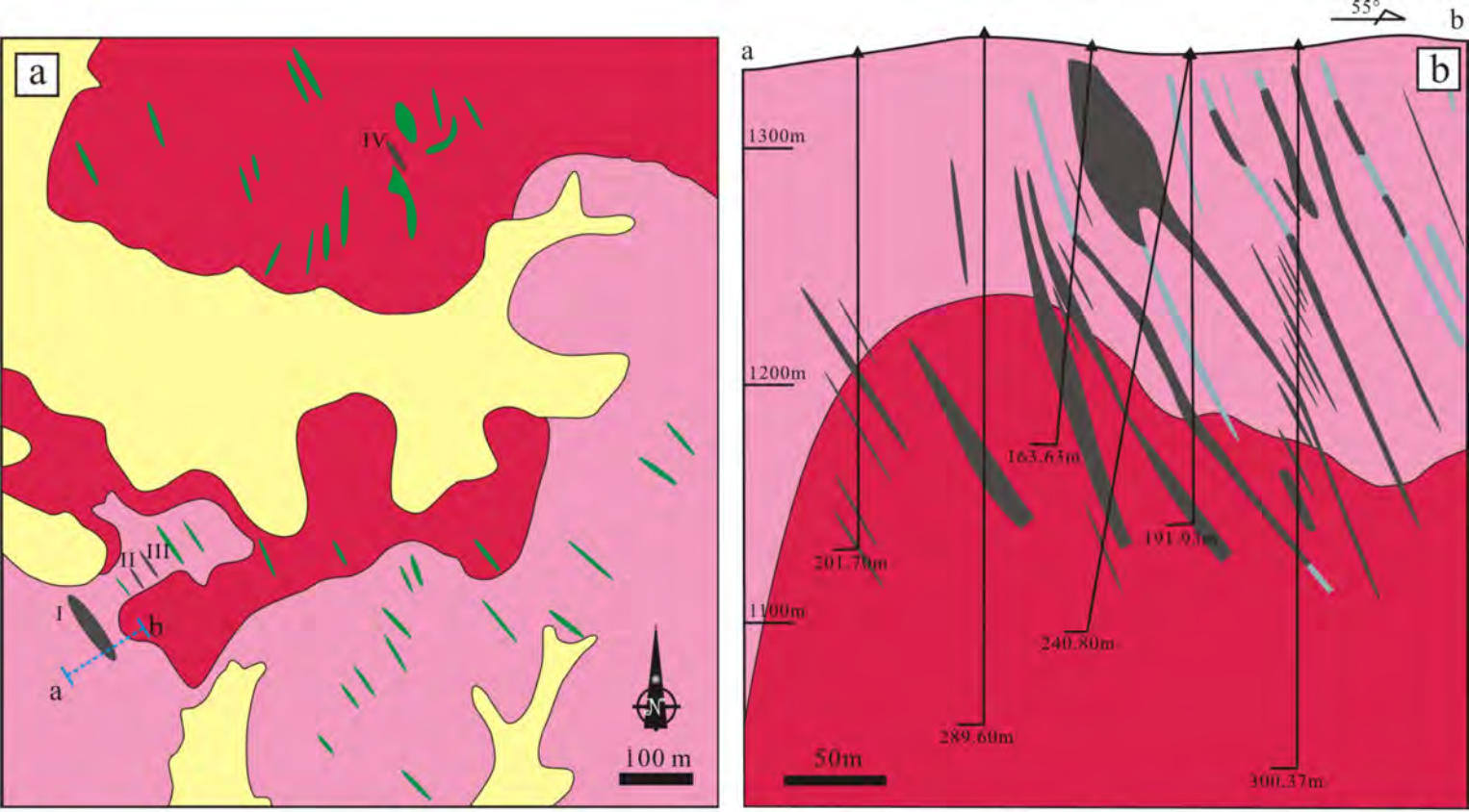

Zhai, D. G., J. J. Liu, S. Tombros, and A. E. Williams-Jones. "The Genesis of the Hashitu Porphyry Molybdenum Deposit, Inner Mongolia, Ne China: Constraints from Mineralogical, Fluid Inclusion, and Multiple Isotope (H, O, S, Mo, Pb) Studies." Mineralium Deposita 53, no. 3 (Mar 2018): 377-97. http://dx.doi.org/10.1007/s00126-017-0745-5.

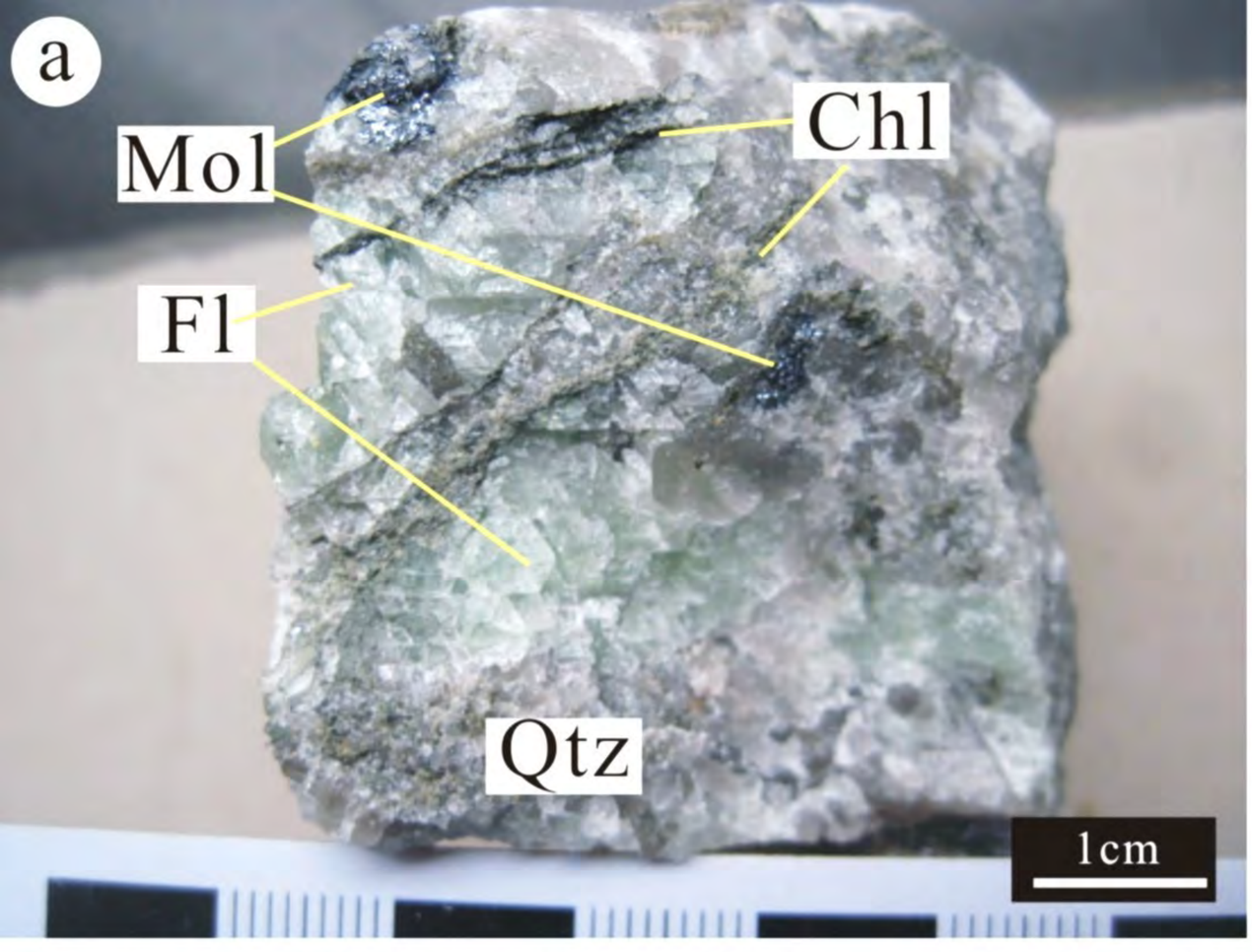

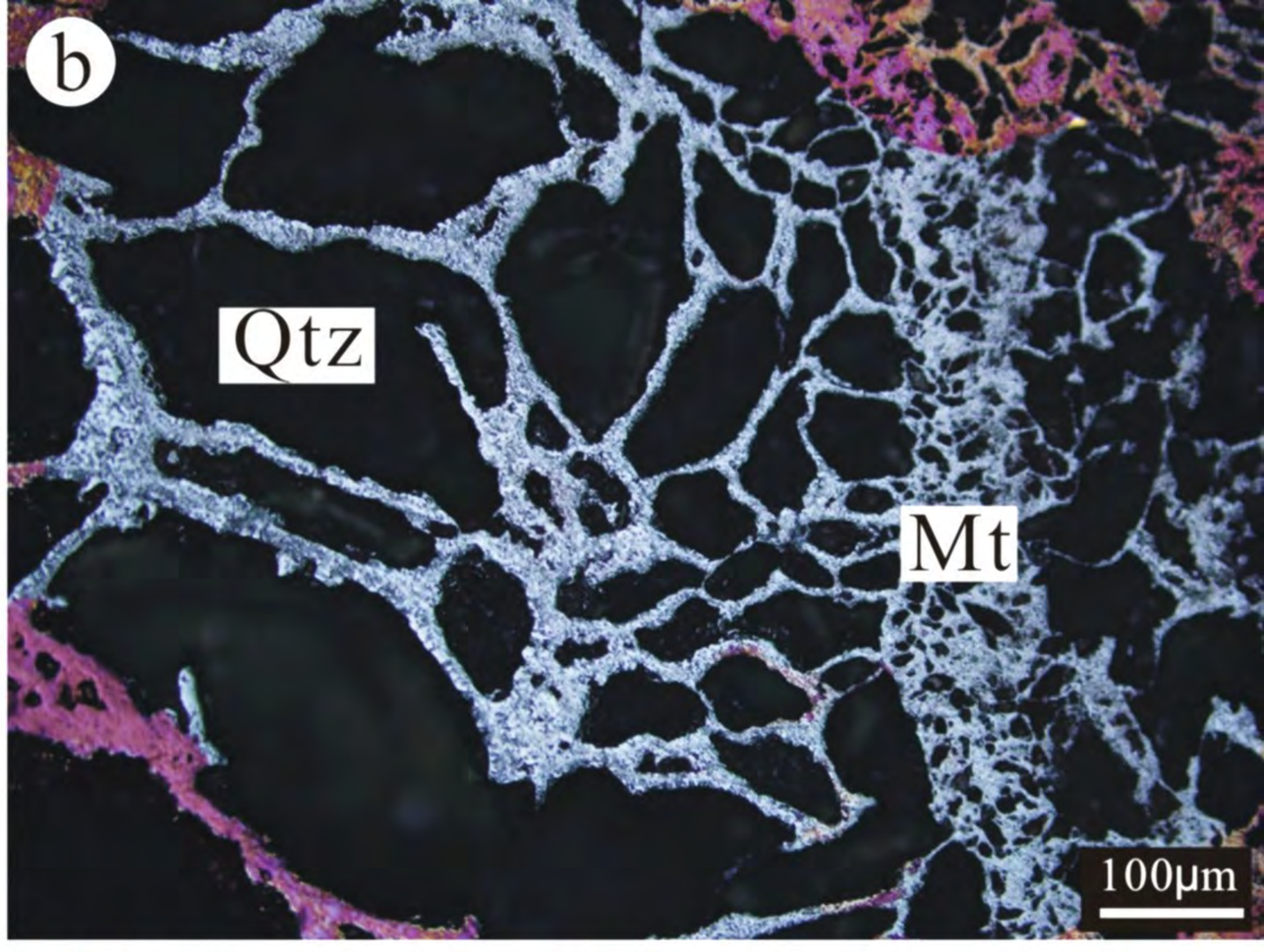

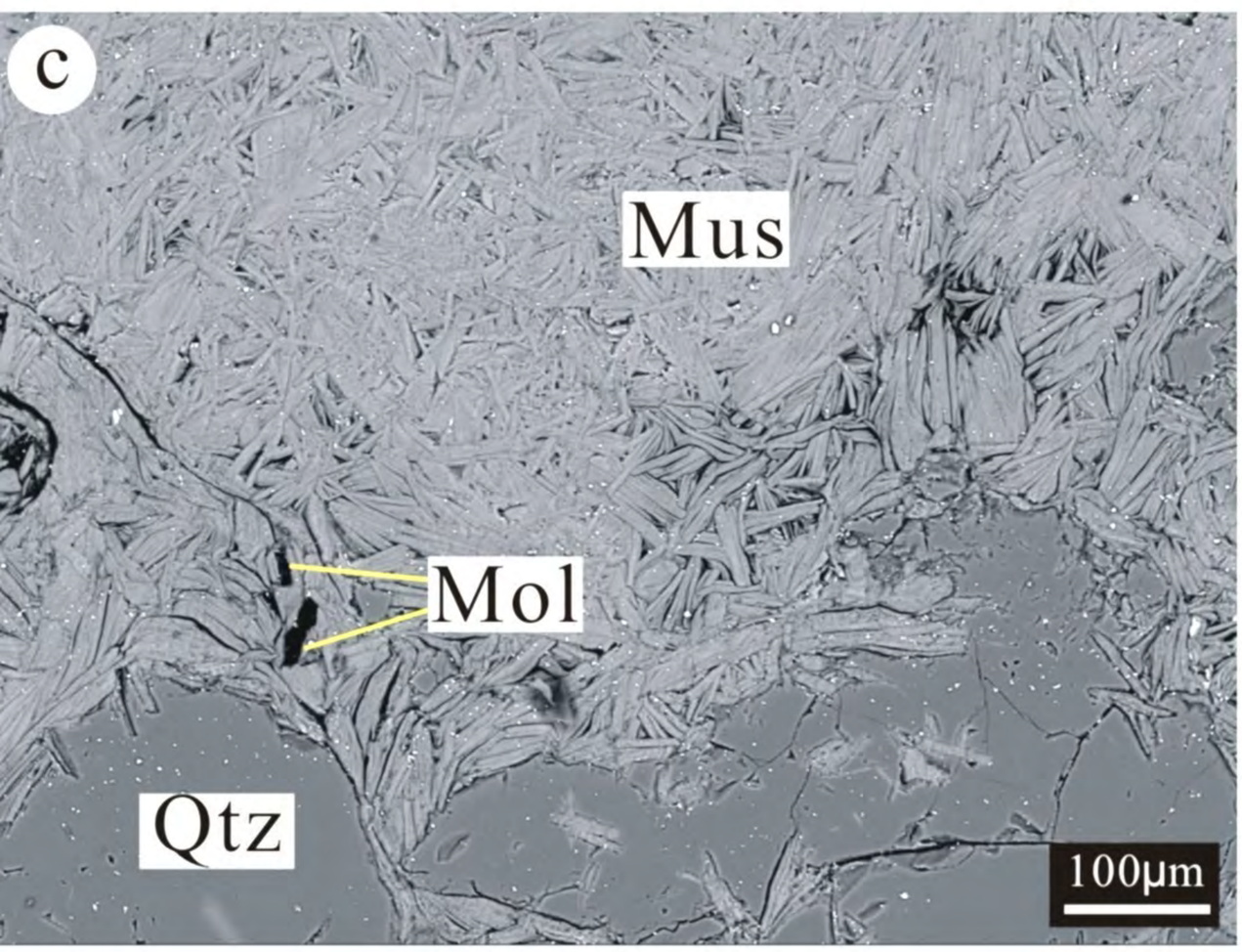

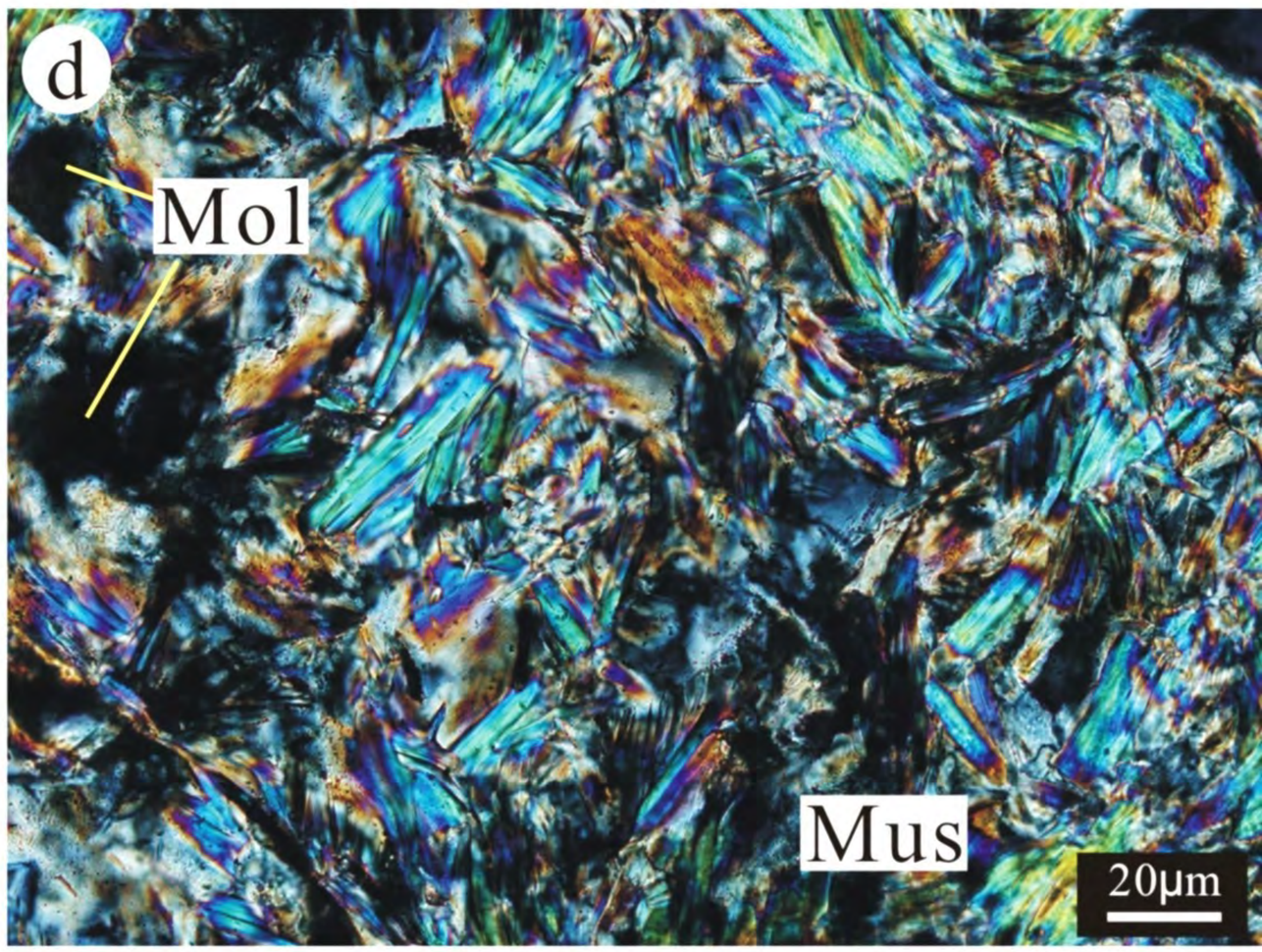

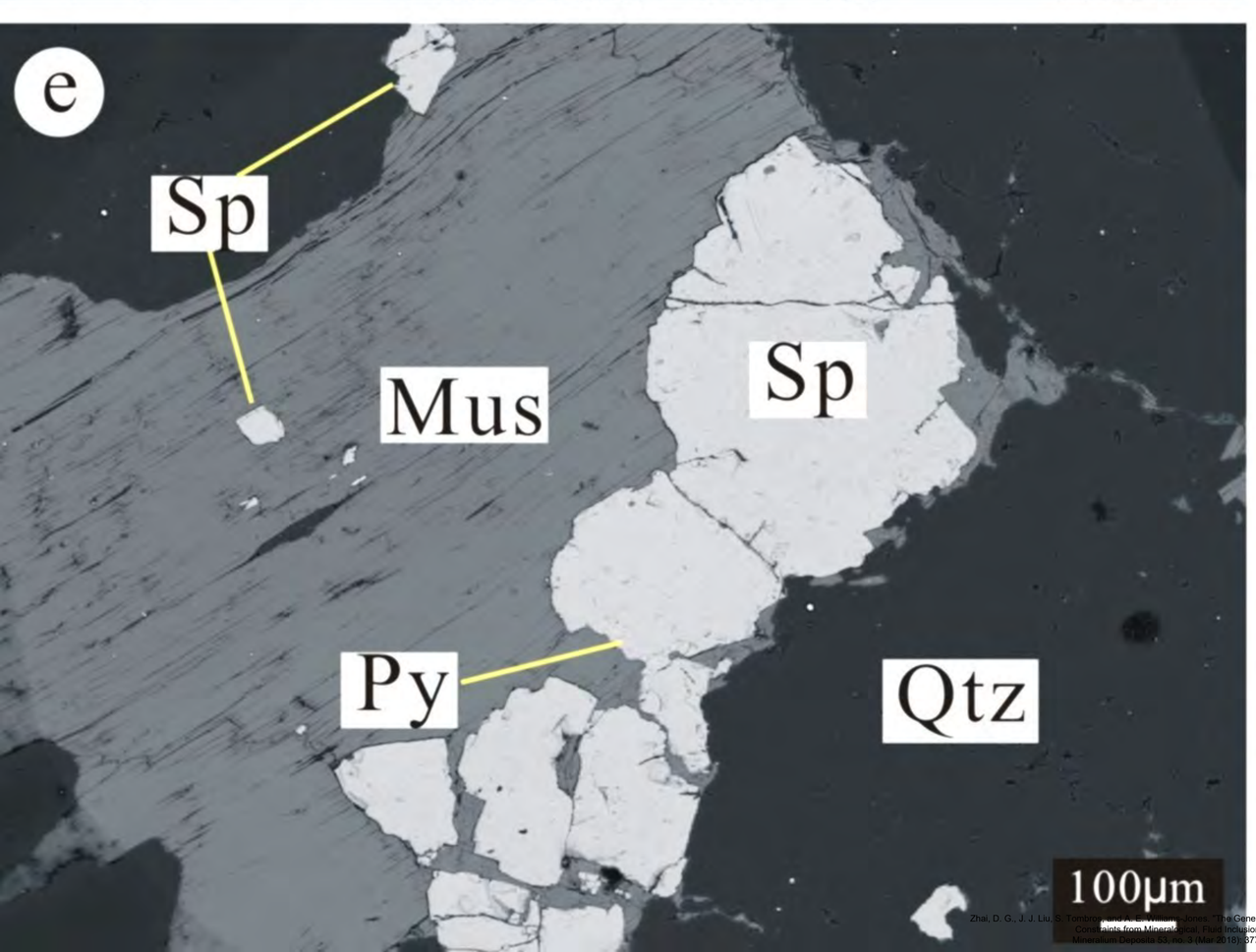

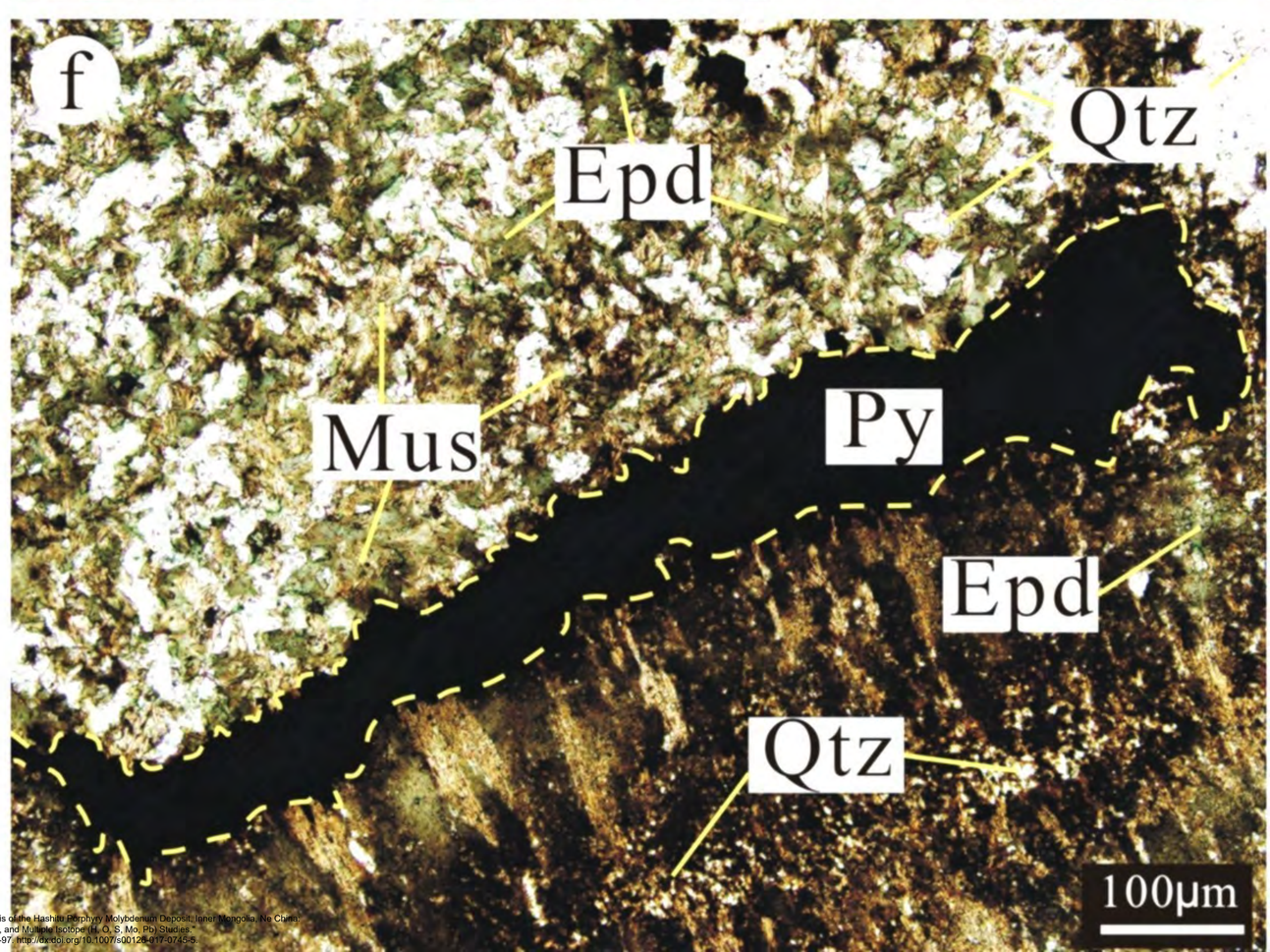

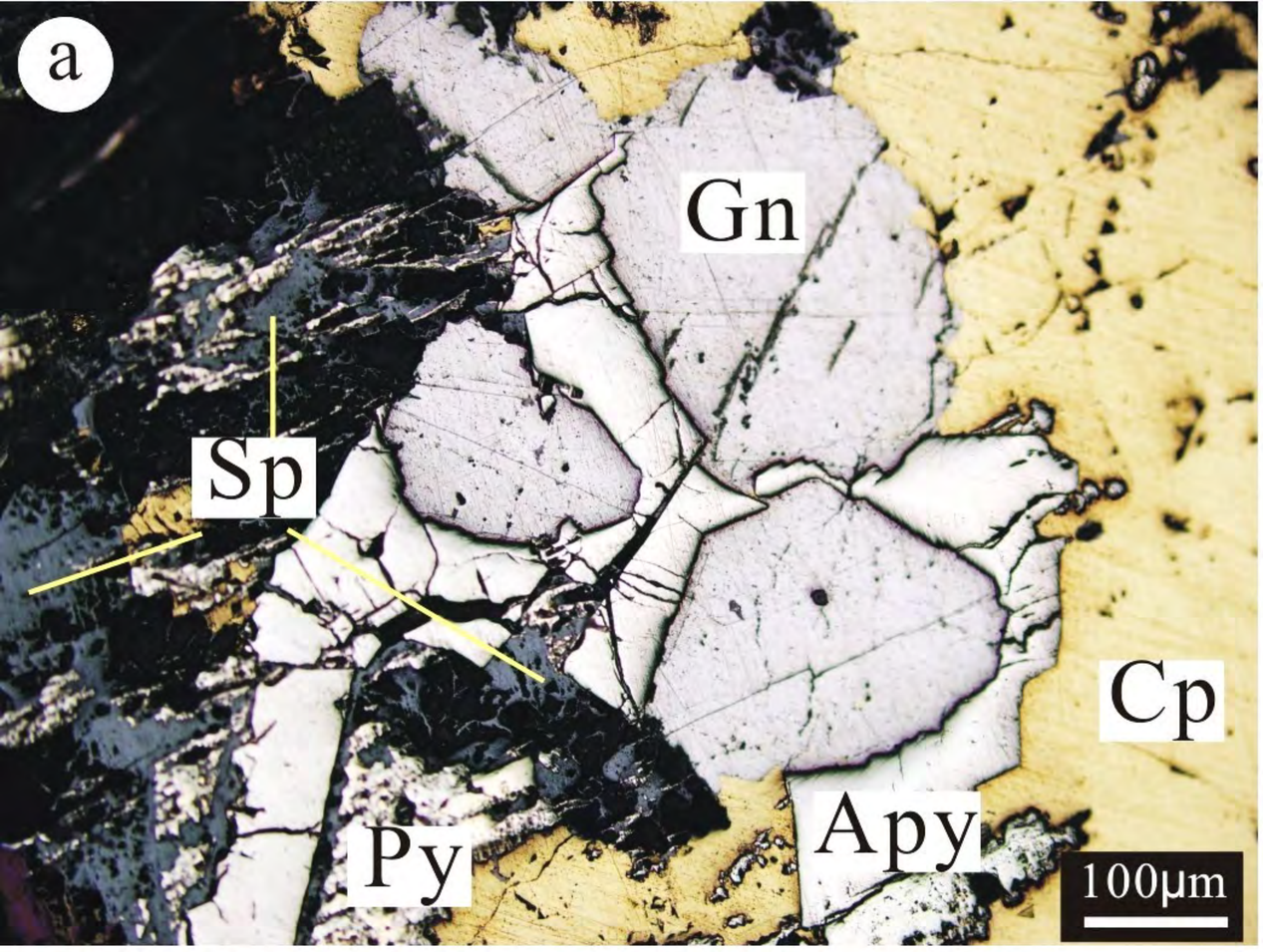

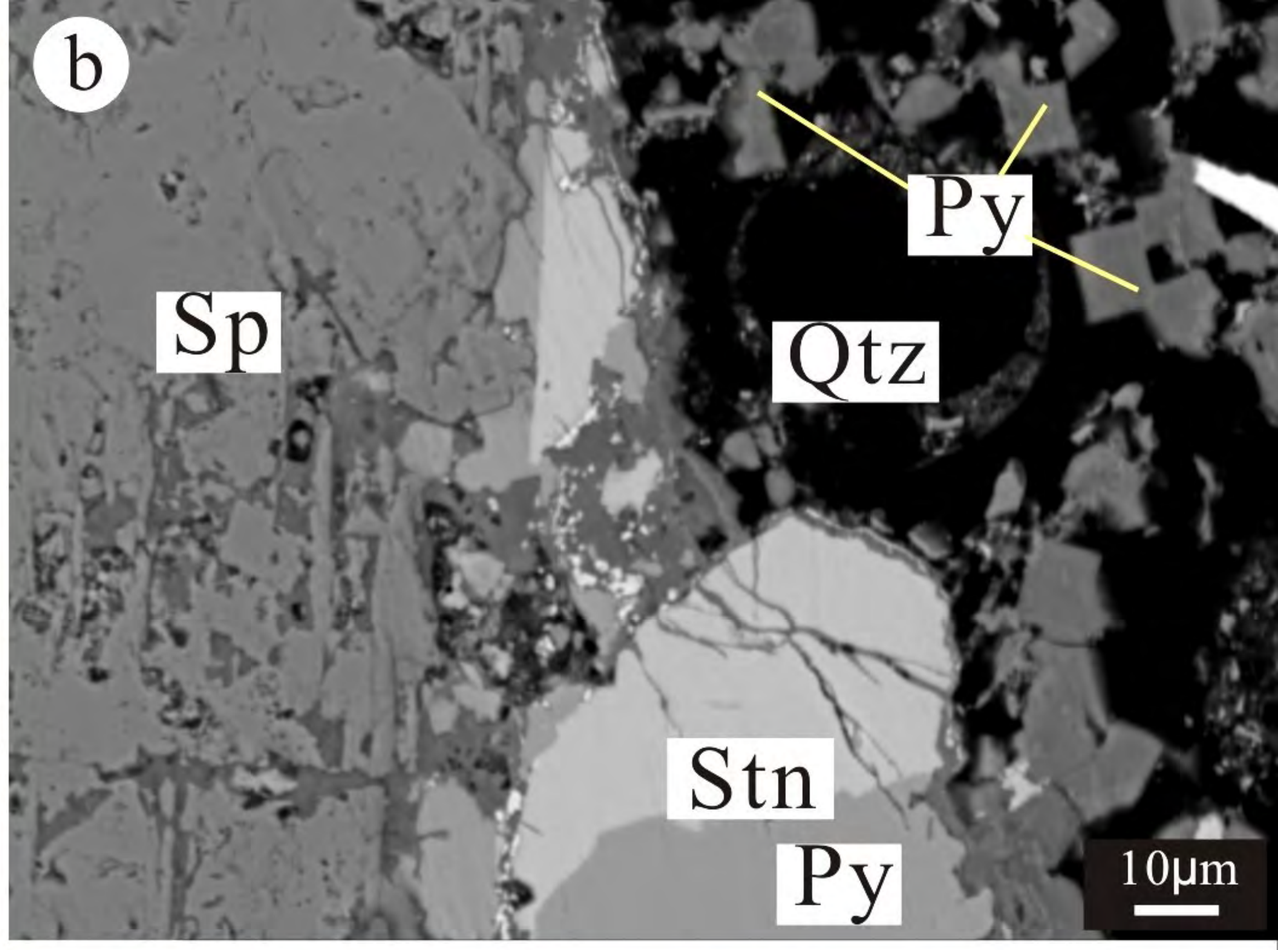

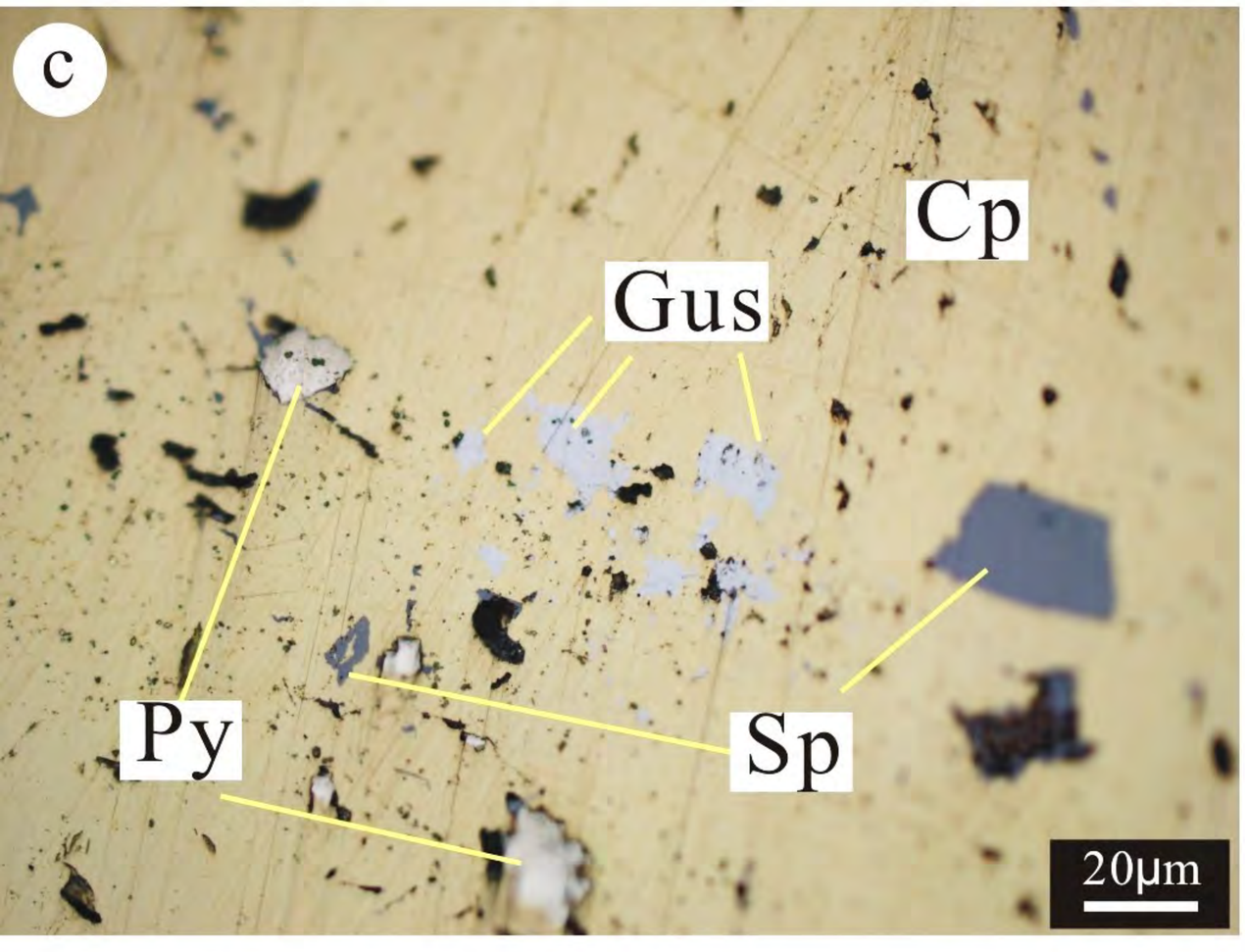

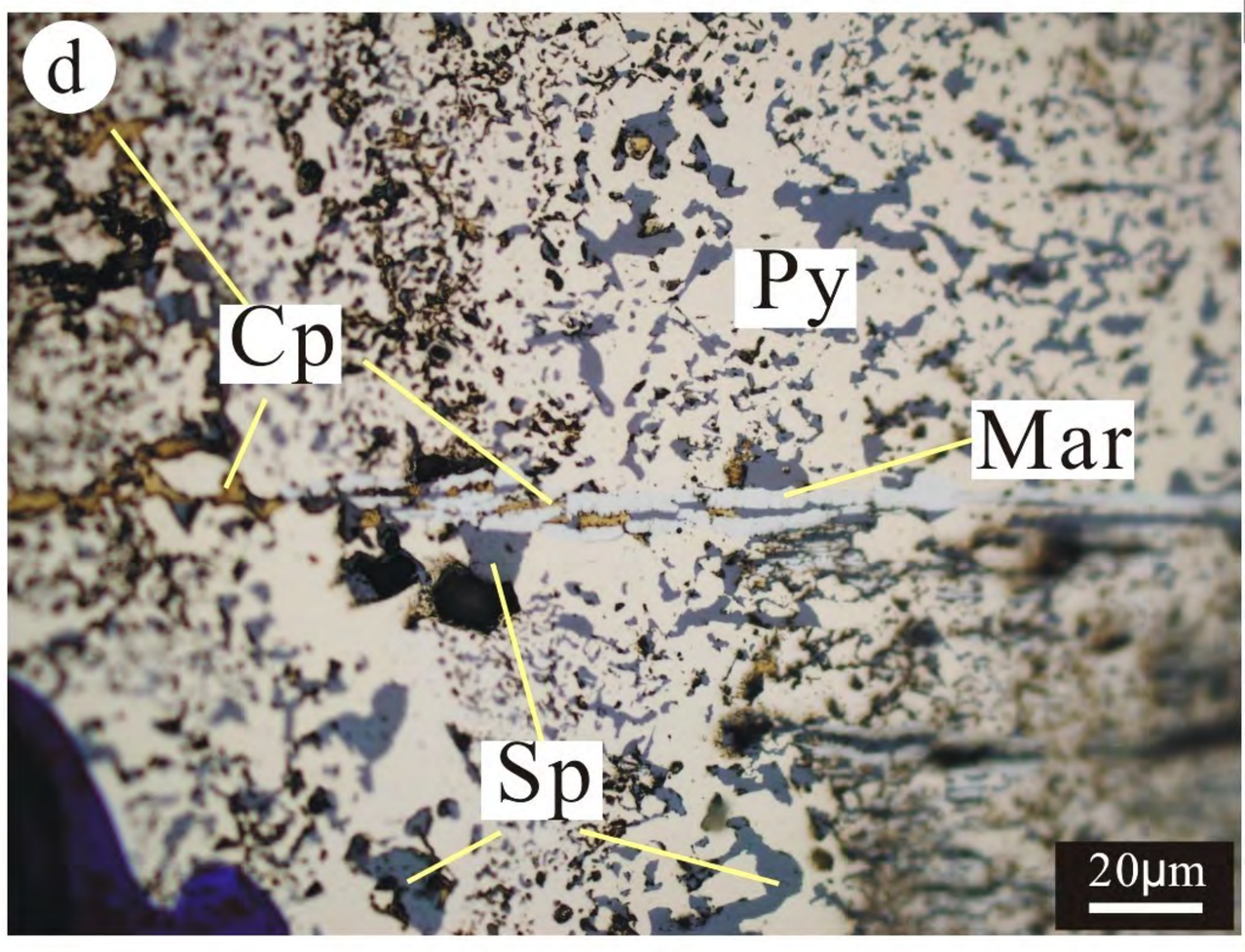

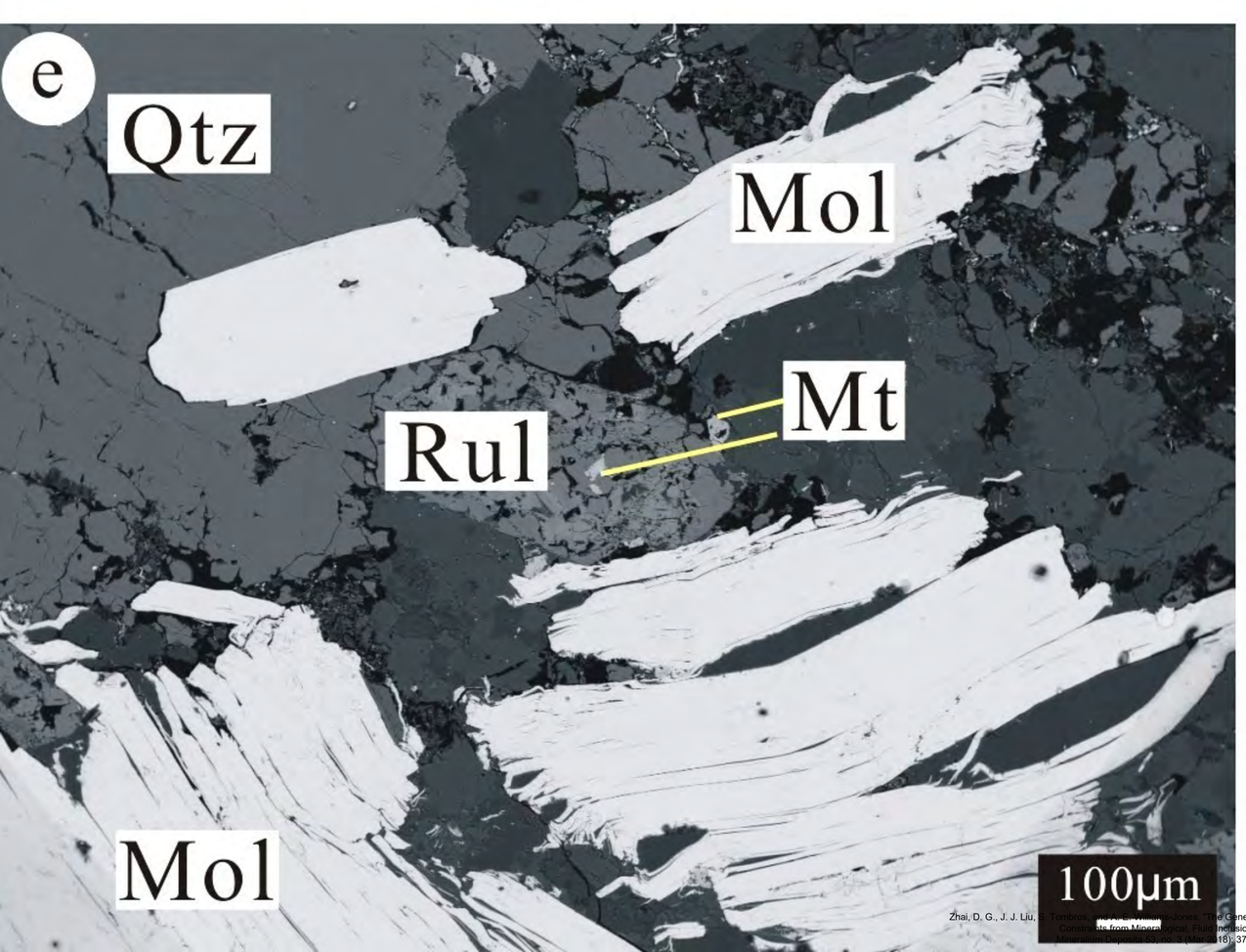

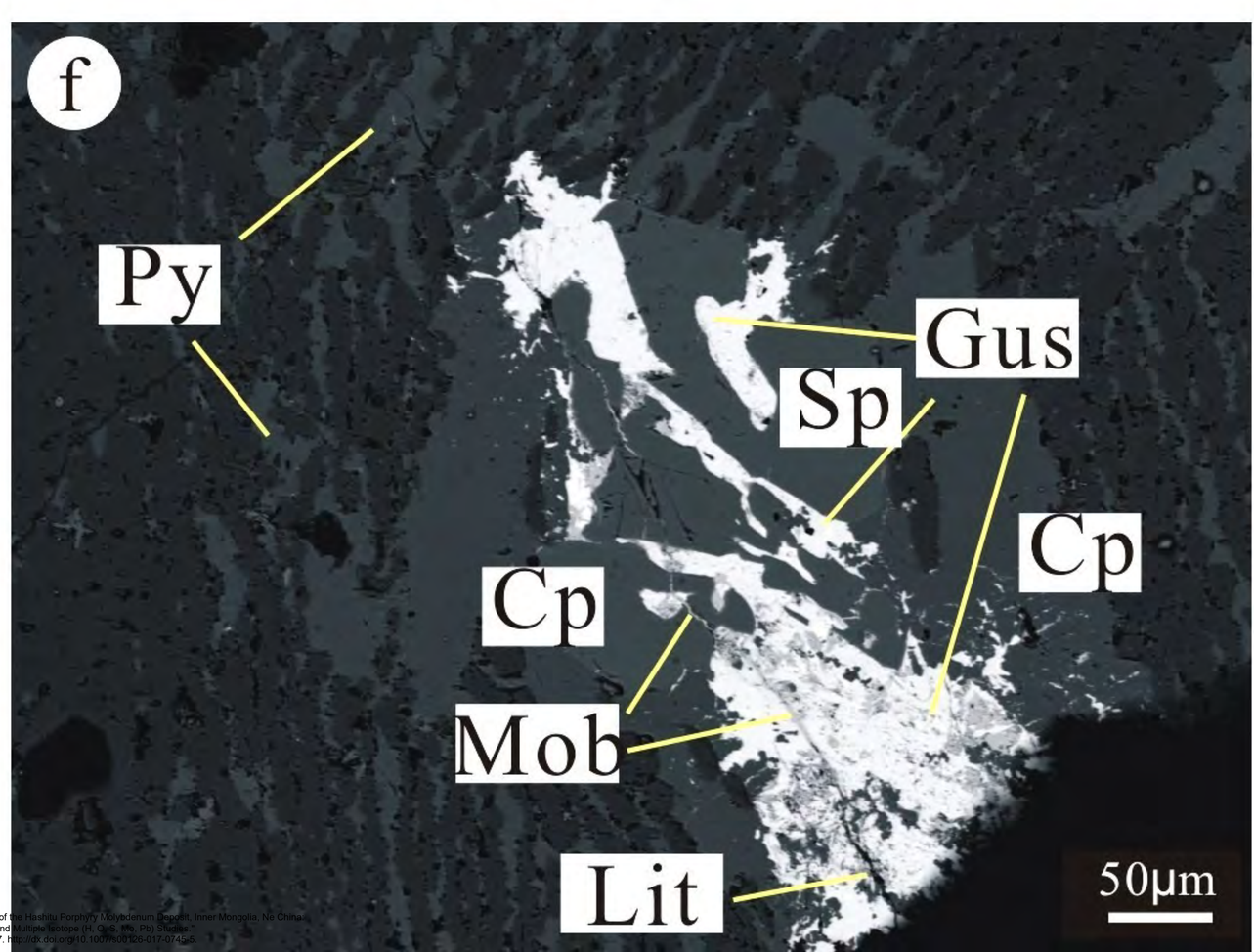

5mm

2.9 3.0
gn cp
a
2.5
py
2.4
py
2.3
py
2.5 2.3
gn py
2.4
2.4
2.6
2.5
2.1
py
2.8 2.8 2.0
cp cp py

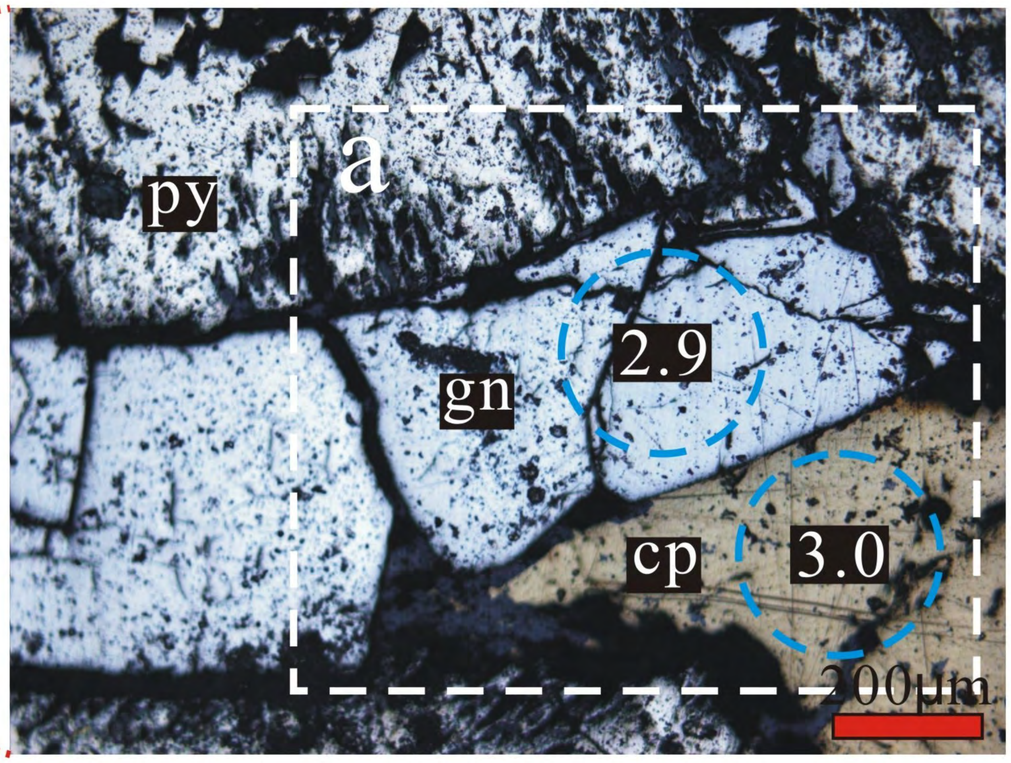

1.7 2.1
cp mol
qtz
py
5mm

2.7
py
2.6
py
2.3
py
2.0
py
c
2.6 py
1.9
cp
2.6 2.4
py cp
5mm

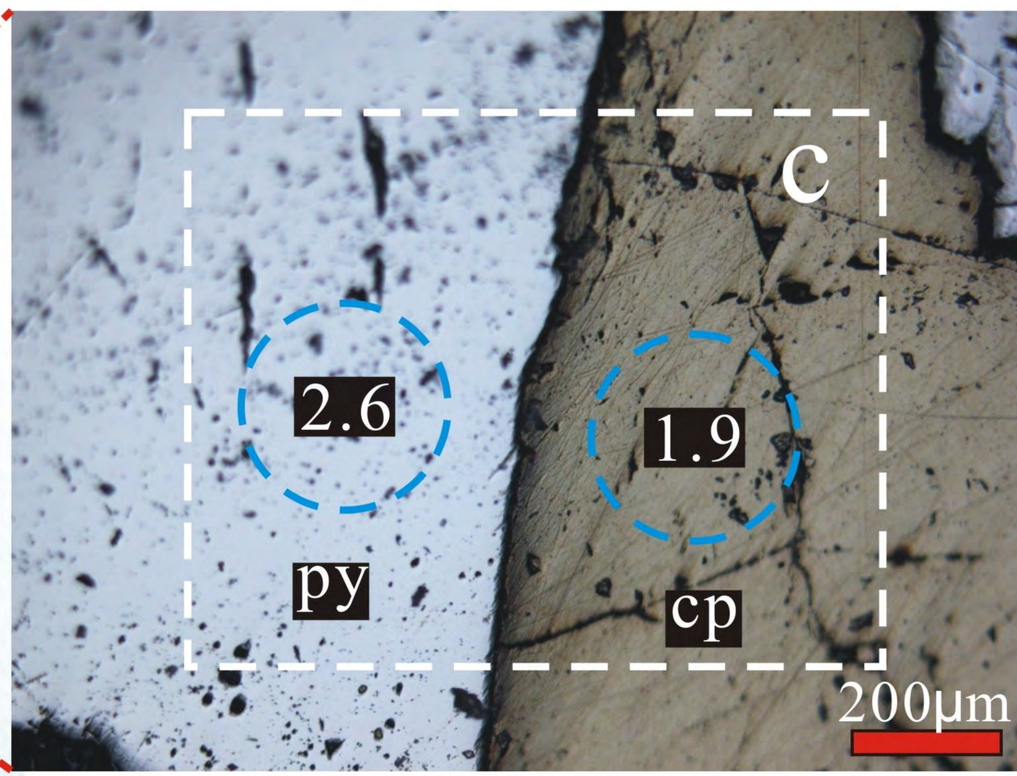

Zhai, D. G., J. J. Liu, S. Tombros, and A. E. Williams-Jones. "The Genesis of the Hashitu Porphyry Molybdenum Deposit, Inner Mongolia, Ne China: Constraints from Mineralogical, Fluid Inclusion, and Multiple Isotope (H, O, S, Mo, Pb) Studies." Mineralium Deposita 53, no. 3 (Mar 2018): 377-97. http://dx.doi.org/10.1007/s00126-017-0745-5.

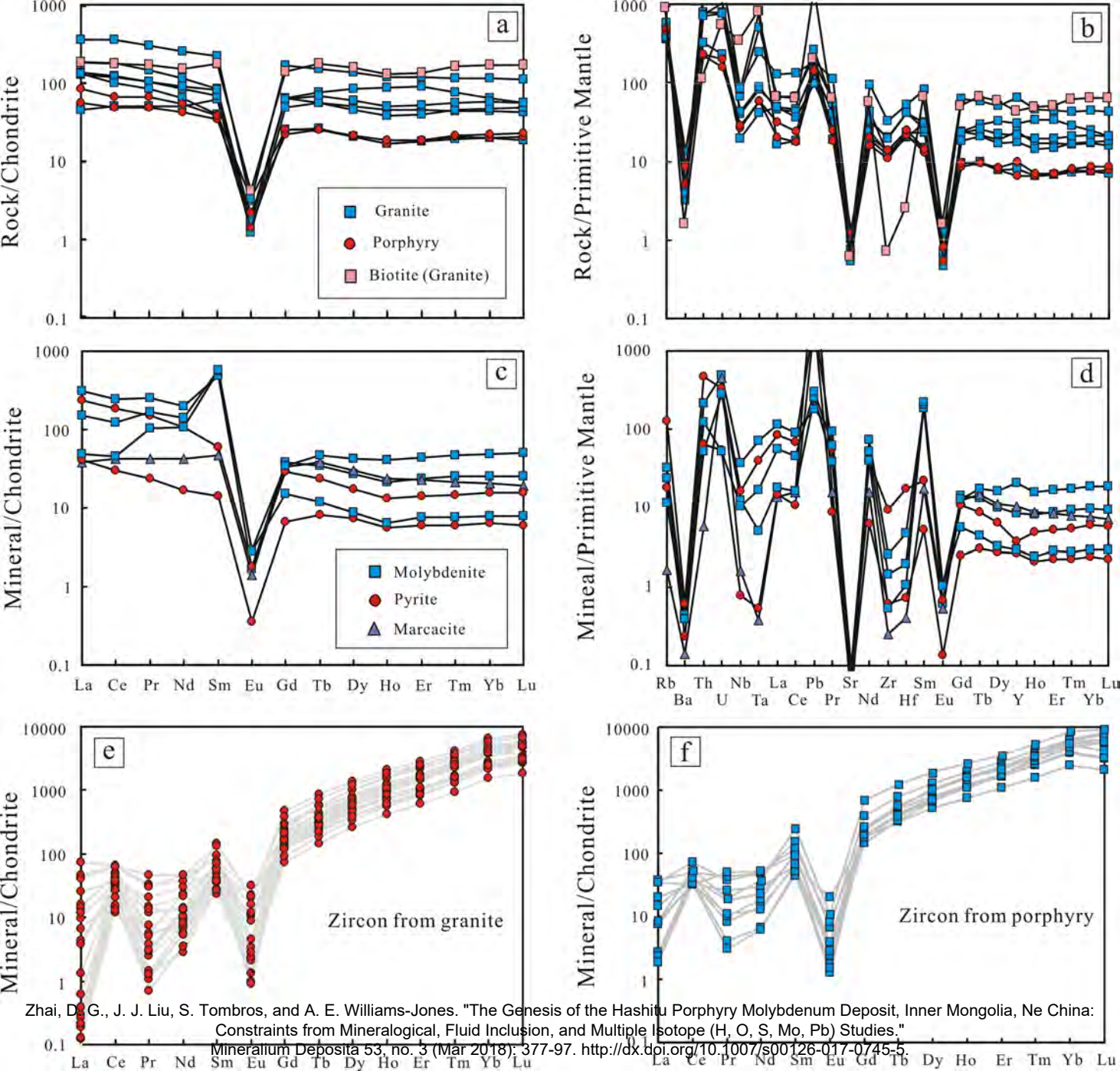

Zhai, D. G., J. J. Liu, S. Tombros, and A. E. Williams-Jones. "The Genesis of the Hashitu Porphyry Molybdenum Deposit, Inner Mongolia, NE China: Constraints from Mineralogical, Fluid Inclusion, and Multiple Isotope (H, O, S, Mo, Pb) Studies." Mineralium Deposita 53, no. 3 (Mar 2018): 377-97. http://dx.doi.org/10.1007/s00126-017-0745-5.

a

L-V

20μm

b

V-L

V

L-V

L-V-S

20μm

c

V

10μm

d

V-L

L-V-S

L-V

50μm

e

L-V-S

L

L-V

L-V

20μm

f

Hem

L-V

L-V-S

V

20μm

g

L-V-S

Mol

20μm

h

50μm

M

i

L-V-S

L

L-V-S

20μm

Zhai, D. G., J. J. Liu, S. Tombros, and A. E. Williams-Jones. "The Genesis of the Hashitu Porphyry Molybdenum Deposit, Inner Mongolia, Ne China: Constraints from Mineralogical, Fluid Inclusion, and Multiple Isotope (H, O, S, Mo, Pb) Studies." Mineralium Deposita 53, no. 3 (Mar 2018): 377-97. http://dx.doi.org/10.1007/s00126-017-0745-5.

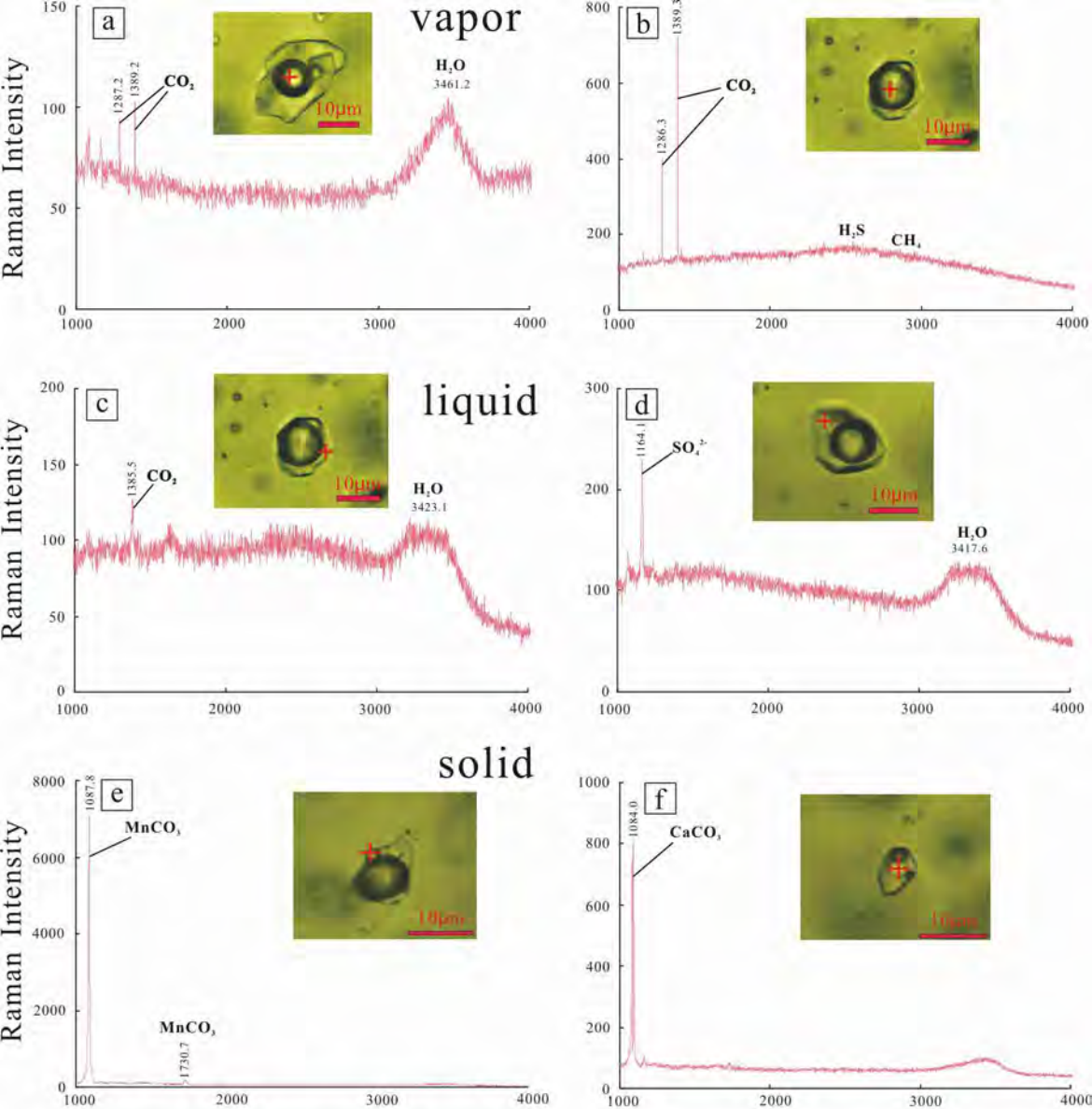

J. J. Liu, S. Tombros, and A. E. Williams-Jones. "The Genesis of the Hashitu Porphyry Molybdenum Deposit, Inner Mongolia Constraints from Mineralogical, Fluid Inclusion, and Multiple Isotope (H, O, S, Mo, Pb) Studies." Mineralium Deposita 53, no. 3 (Mar 2018): 377-97. http://dx.doi.org/10.1007/s00126-017-0745-5.

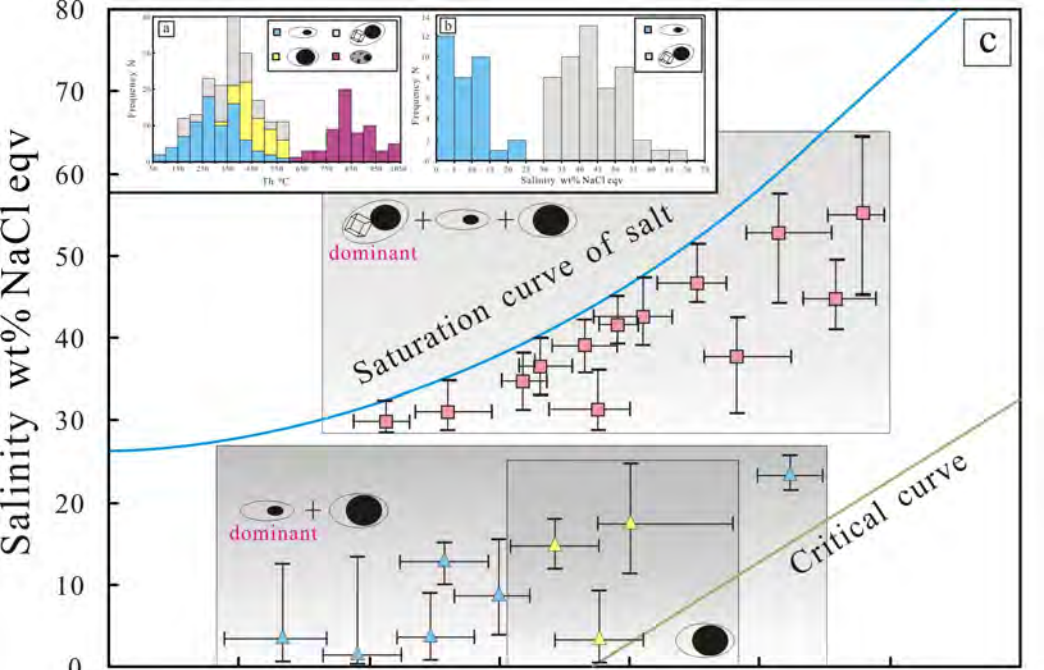

u, S. Tombros, and A. E. Williams-Jones. "The Genesis of the Hashitu Porphyry Molybdenum Deposit, Inner M
Constraints from Mineralogical, Fluid Inclusion, and Multiple Isotope (H, O, S, Mo, Pb) Studies."
Mineralium Deposita 53, no. 3 (Mar 2018): 377-97. http://dx.doi.org/10.1007/s00126-017-0745-5.

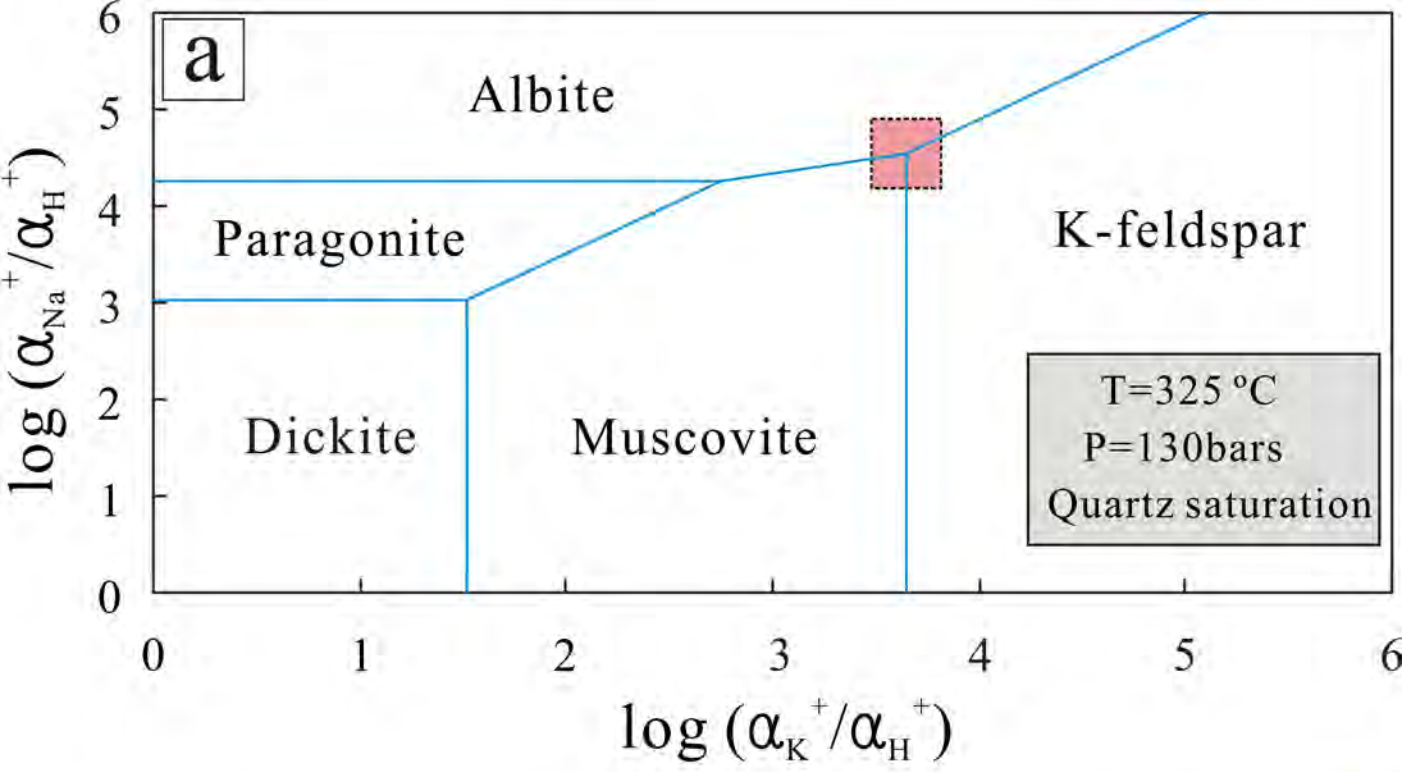

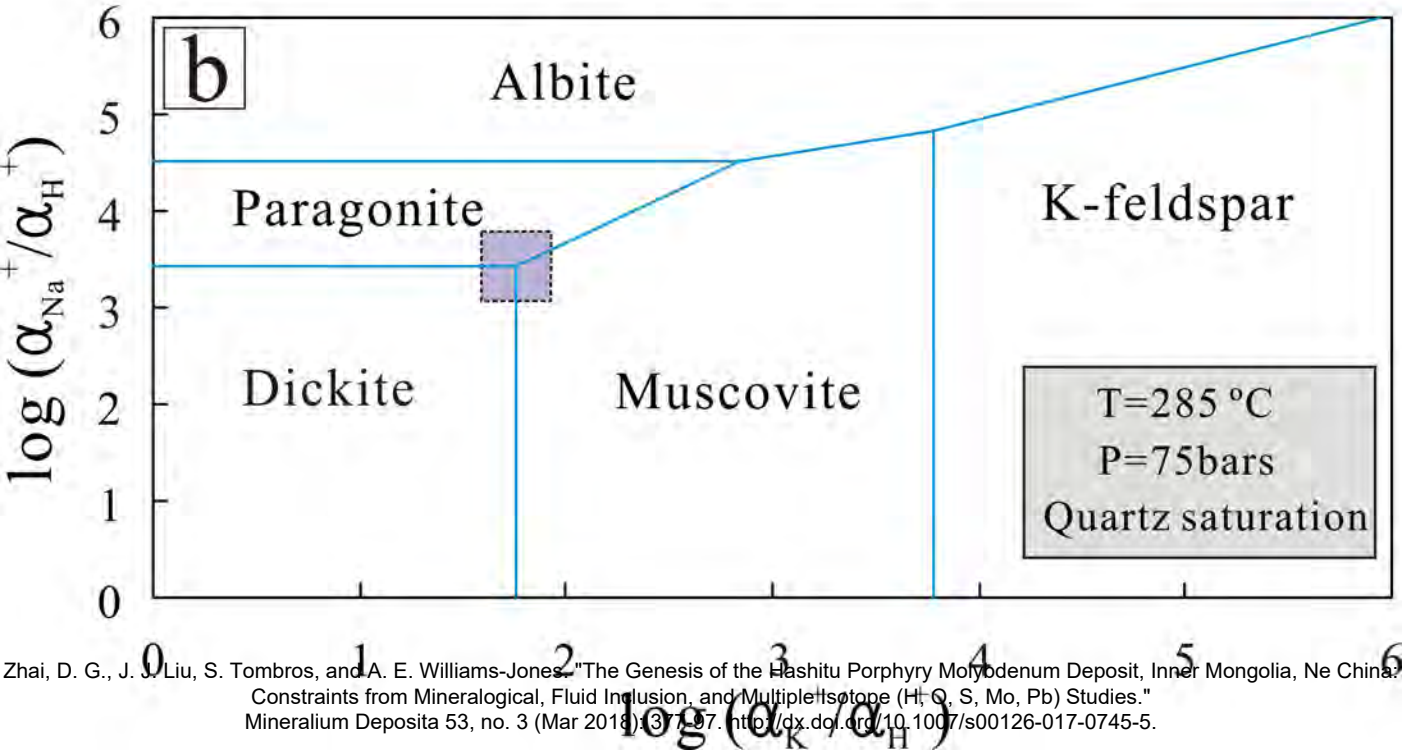

Zhai, D. G., J. J. Liu, S. Tombros, and A. E. Williams-Jones. "The Genesis of the Hashitu Porphyry Molybdenum Deposit, Inner Mongolia, Ne China: Constraints from Mineralogical, Fluid Inclusion, and Multiple Isotope (H, O, S, Mo, Pb) Studies." Mineralium Deposita 53, no. 3 (Mar 2018): 377-97. http://dx.doi.org/10.1007/s00126-017-0745-5.

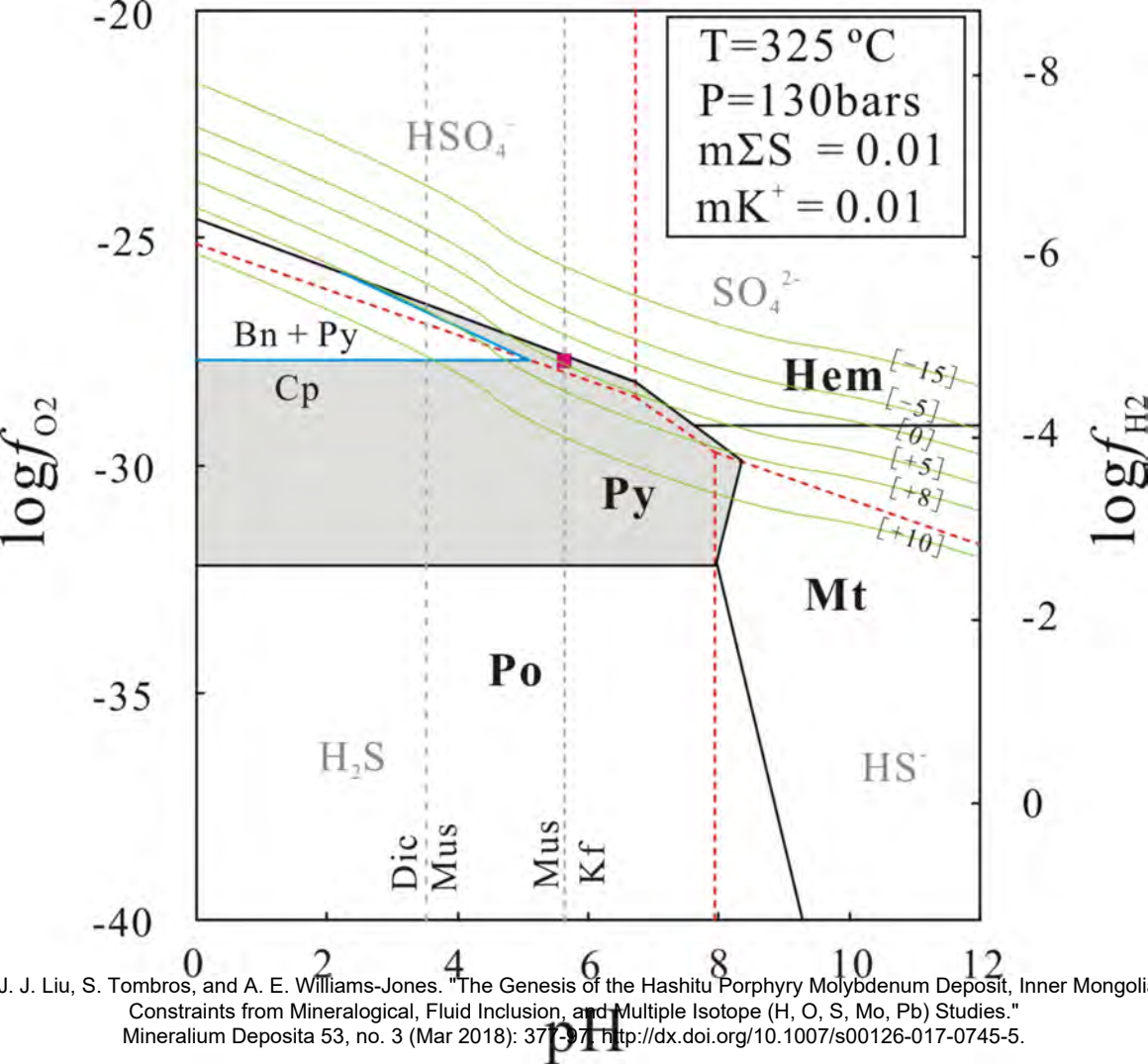

J. J. Liu, S. Tombros, and A. E. Williams-Jones. "The Genesis of the Hashitu Porphyry Molybdenum Deposit, Inner Mongoli
Constraints from Mineralogical, Fluid Inclusion, and Multiple Isotope (H, O, S, Mo, Pb) Studies."
Mineralium Deposita 53, no. 3 (Mar 2018): 377-97. http://dx.doi.org/10.1007/s00126-017-0745-5.

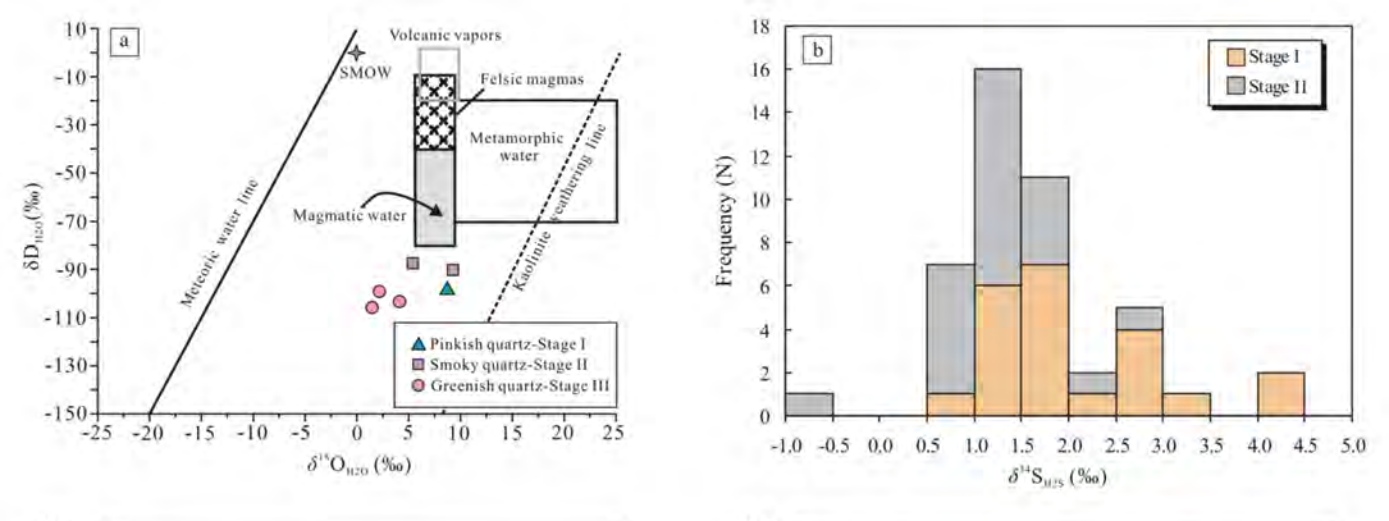

Zhai, D. G., J. J. Liu, S. Tombros, and A. E. Williams-Jones. "The Genesis of the Hashitu Porphyry Molybdenum Deposit, Inner Mongolia, NE China: Constraints from Mineralogical, Fluid Inclusion, and Multiple Isotope (H, O, S, Mo, Pb) Studies." Mineralium Deposita 53, no. 3 (Mar 2018): 377-97. http://dx.doi.org/10.1007/s00126-017-0745-5.

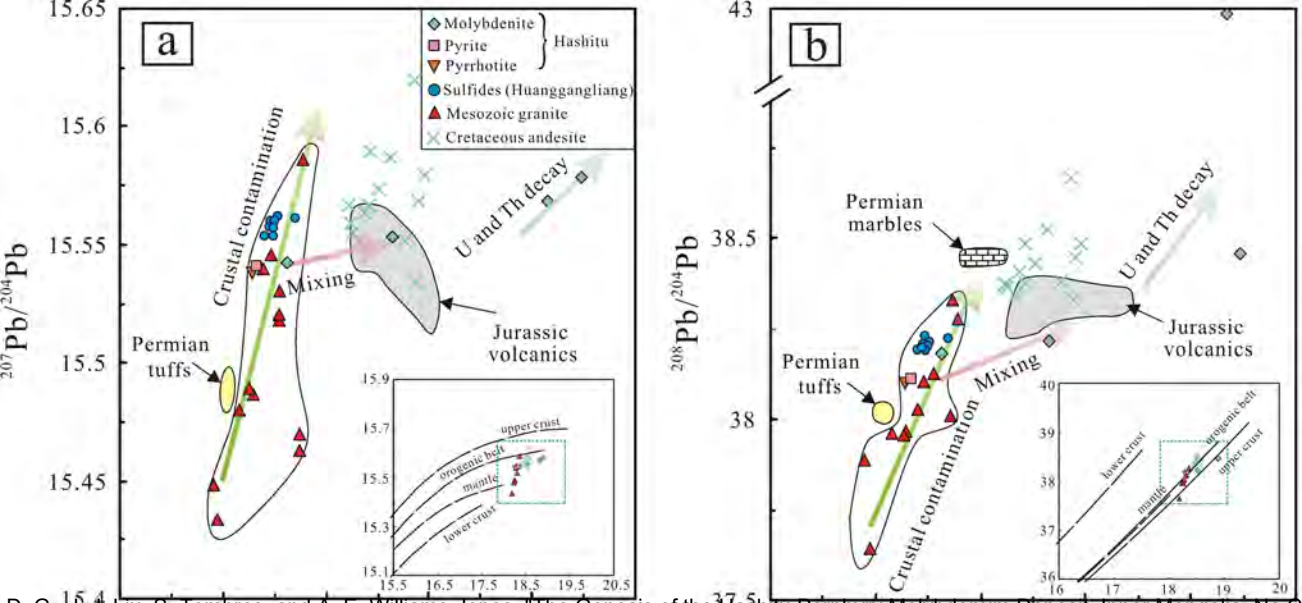

D. G., J. J. Liu, S. Tombros, and A. E. Williams-Jones. "The Genesis of the Hashitu Porphyry Molybdenum Deposit, Inner Mongolia, NE C
Constraints from Mineralogical, Fluid Inclusion, and Multiple Isotope (H, O, S, Mo, Pb) Studies."
Mineralium Deposita 53, no. 3 (Mar 2018): 377-97. http://dx.doi.org/10.1007/s00126-017-0745-5.